Distribution Agreement

In presenting this thesis as a partial fulfillment of the requirements for a degree from Emory University, I hereby grant to Emory University and its agents the non-exclusive license to archive, make accessible, and display my thesis in whole or in part in all forms of media, now or hereafter now, including display on the World Wide Web. I understand that I may select some access restrictions as part of the online submission of this thesis. I retain all ownership rights to the copyright of the thesis. I also retain the right to use in future works (such as articles or books) all or part of this thesis.

Yiran Zhang April 12, 2022

Synthesis, Characterization, and Preliminary Oxidative Reactivity Study of Two Novel Cu Complexes with a Tripodal Amidate Ligand

by

Yiran Zhang

Cora MacBeth
Adviser

Chemistry

Cora MacBeth

Adviser

Austin Scharf

Committee Member

Matthew Weinschenk

Committee Member

Effrosyni Seitaridou

Committee Member

2022

Synthesis, Characterization, and Preliminary Oxidative Reactivity Study of Two Novel Cu Complexes with a Tripodal Amidate Ligand

By

Yiran Zhang

Cora MacBeth

Adviser

An abstract of
a thesis submitted to the Faculty of Emory College of Arts and Sciences
of Emory University in partial fulfillment
of the requirements of the degree of
Bachelor of Science with Honors

Chemistry

2022

Abstract

Synthesis, Characterization, and Preliminary Oxidative Reactivity Study of Two Novel Cu Complexes with a Tripodal Amidate Ligand

By Yiran Zhang

Oxidation reactions are an important class of chemical reactions. With the consideration that many traditional oxidants tend to generate much chemical waste, efforts have been devoted to developing catalysts that can activate O_2 as a more sustainable oxidant. Cu-centered oxidases and oxygenases are crucial models for designing O_2-activation catalysts. Among the O_2-activating Cu centers found in nature, a specific type features a mononuclear Cu center with a non-planar, histidine-rich coordination environment, such as the active sites in peptidylglycine-α-hydroxylating monooxygenase (PHM) and Cu amine oxidase (CAO). To simulate the O_2 reactivity of such Cu centers, many synthetic Cu complexes bearing tripodal ligands with four coordinating nitrogen atoms (tripodal-N_4 Cu complexes) have been prepared and studied as modeling compounds. Despite the abundant investigations made in this field, all the reported tripodal-N_4 ligands are neutral. Therefore, with the purpose to expand the scope of tripodal-N_4 Cu complexes available as candidate catalysts for O_2 utilization, a redox pair of Cu complexes supported by an anionic amidate ligand $N(o\text{-}PhNHC(O)CF_3)_3$ are prepared in the current study.

In chapter 2 of the thesis, synthesis, characterization, and preliminary oxidative reactivity of $(PPh_4)_2[Cu(N(o\text{-}PhNC(O)CF_3)_3)]$ (1) and $PPh_4[Cu(N(o\text{-}PhNC(O)CF_3)_3)]$ (2) are presented. Both complexes are produced in high yields, and their solid-state characterization reveals unusual structural features which can be attributed to the charged ligand backbone. The solution-state behavior of the two complexes cannot be unambiguously described so far. The reaction of complex 1 with O_2 at room temperature displays a reaction profile inconsistent with the previously established pathway where a Cu(II)-superoxo intermediate is involved, and several postulates are proposed.

In the same chapter, two unexpected discoveries made in this study are also included: first, a transformation of PPh_4^+ to $P(O)Ph_3$ is detected while reacting complex 1 with Et_4NCN, and kinetic experiments indicate the positive roles of O_2 and Et_4NCN; second, hydroxylation-defluorination of the ligand backbone in complex 2 is observed while optimizing the preparation of complex 2. Curiosity into these two findings and other unresolved results in the current study raises several questions for future research.

Synthesis, Characterization, and Preliminary Oxidative Reactivity Study of Two Novel Cu Complexes with a Tripodal Amidate Ligand

By

Yiran Zhang

Cora MacBeth

Adviser

A thesis submitted to the Faculty of Emory College of Arts and Sciences
of Emory University in partial fulfillment
of the requirements of the degree of
Bachelor of Science with Honors

Chemistry

2022

Acknowledgements

I would like to thank everyone in the MacBeth lab who has helped me during my two years of undergraduate research experience: Dr. Cora MacBeth as a patient and encouraging mentor, Dr. Elaine Liu as my graduate student mentor in my junior year, as well as Ailing Yu and Annabel Zhang as highly supportive colleagues.

Also, I am grateful for the help provided by Dr. John Bacsa from Emory X-ray crystallography center and Dr. Bing Wang from Emory NMR research center. Without their assistance, it would not be possible for me to identify the structures and carry out the kinetic experiments indispensable for making the exciting discoveries in my project.

Besides, I wish to express my thanks to my thesis committee members: Dr. Austin Scharf and Dr. Effrosyni Seitaridou at Oxford College, as well as Dr. Matthew Weinschenk at Emory College. Being excellent instructors, they have played significant roles at different stages of my undergraduate career in making me grow as a chemist and as a scientist.

Lastly, I am in deep gratitude to my friends and families who are always there for me, although for many of them we do not see each other very often recently. Their unconditional love and confidence in me have sustained me through the past two years of isolated life in the middle of COVID-19 and have given me the courage to deal with any challenges.

Table of Contents

Chapter 1. Development of Tripodal-N_4 Cu Complexes Modelling Cu-centered Oxygenases and Oxidases Reactivity

Introduction

Oxidation is an important type of reactions in chemistry, and recently there is a growing demand in rendering this class of reactions more environmentally friendly due to the large amounts of chemical waste generated by traditional strong oxidants such as potassium permanganate ($KMnO_4$), chromic acid (H_2CrO_4), and pyridinium chlorochromate (PCC), etc. As more sustainable oxidants are looked for, dioxygen (O_2) becomes a decent candidate since it will be reduced to hydrogen peroxide (H_2O_2) and water (H_2O), which are both environmentally benign.[1] One viable approach of investigating the potential of O_2 as an effective oxidant is through understanding and simulating the catalytic reactivity of oxygenase and oxidase systems in nature using synthesized compounds.

A great number of oxygenases and oxidases feature one or more copper centers at their active sites. Thus, in the past decades many Cu complexes have been synthesized to mimic these enzymes' O_2 activating abilities.[1, 2] A particular type of such complexes are mononuclear Cu complexes supported by tripodal ligands with four coordinating nitrogen atoms (tripodal-N_4 ligands), which are especially useful for modelling the reactivity of any mononuclear O_2 activation Cu centers in nature.

In this chapter, firstly, an overview of the structure and O_2 activating pathways of two illustrative mononuclear enzymic Cu centers in nature will be presented; then, representative attempts in literature that employ tripodal-N_4 Cu complexes to activate O_2 and explore the possible reactive intermediates will be discussed.

Mononuclear O_2 Activating Cu Centers in Nature

Peptidylglycine α-hydroxylating monooxygenase (PHM)/ Dopamine β-monooxygenase(DβM)

PHM and DβM catalyze the hydroxylation of glycine-extended pro-hormones and dopamine, respectively (figure 1-1).[1] Due to sequence homology, conservation of ligands at the Cu active sites, and similar kinetic isotope effects seen in mechanistic studies, PHM and DβM are generally considered to have interchangeable structures and O_2 activation pathways.[3] Early structural characterization of the PHM catalytic core indicates the presence of two non-coupled Cu centers which are 11 Å apart.[4] When both Cu centers are oxidized, the Cu_A site displays square pyramidal geometry with three coordinating δ-histidines and two vacant sites, whereas the Cu_B site shows tetrahedral geometry with two ε-histidines, one methionine, and one H_2O as coordinating ligands (figure 1-2).[4] The reduced catalytic core of PHM has a very similar structure as its oxidized counterpart and is believed to be formed via a two-electron reduction of the oxidized PHM catalytic core with two ascorbate molecules as the reducing agent (figure 1-3).[5-7]

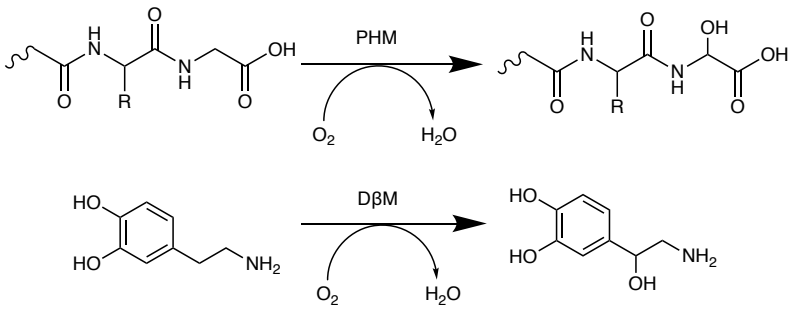

Figure 1-1. Hydroxylation reactions catalyzed by PHM and DβM in nature. In both reactions, O_2 undergoes four-electron reduction to yield H_2O, and a (sp^3)C-H bond in the substrate is substituted with a hydroxyl group. Figure adapted from reference 1.

X-ray crystallographic characterization of a precatalytic PHM complex reveals the role of the reduced Cu_B as the O_2 activation site and the existence of an end-on η^1 Cu_B-O_2 species as O_2

replaces the H_2O ligand on Cu_B(I) (figure 1-3).[6] For many years, while there has been a consensus that an end-on η^1 Cu_B(II)-superoxo intermediate is involved in the hydroxylation mechanism of PHM/ DβM, other steps within the pathway have remained controversial. In addition to the widely accepted mechanism proposed by Klinman (figure 1-3 blue path), later computational studies suggest other possibilities (figure 1-3 red and magenta paths).[7, 8] A recent crystallographic characterization of human DβM reveals a closed conformation of the catalytic core, in which Cu_A and Cu_B are only 5 Å apart, in addition to the open conformation that is seen in PHM.[7, 9] This finding challenges the traditional "non-coupling" description of the DβM catalytic core and stimulates further investigations into the hydroxylation mechanisms of PHM/DβM (figure 1-3 magenta path).

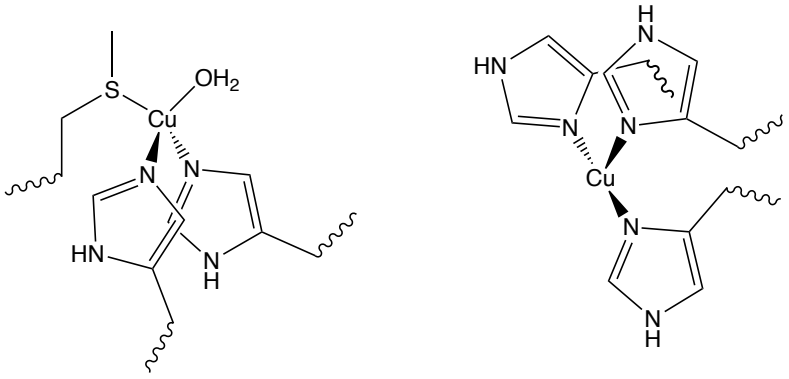

Figure 1-2. The oxidized catalytic core of PHM. The distance between the two non-coupling Cu centers is 11 Å, and this represents the open conformation that is conventionally accepted as the catalytic core structure in PHM/DβM. Cu_A (right) is square pyramidal with its axial and an equatorial position unoccupied; Cu_B (left) is tetrahedral.[4] Figure adapted from reference 4.

Copper Amine Oxidase (CAO)

CAO catalyzes the deamination of primary amines to aldehydes (figure 1-4), and it consists of a Cu center and a 2,4,5-trihyroxyphenylalanine quinone (TPQ) cofactor.[1] Structural characterizations of multiple CAO species show that the Cu center has a distorted square

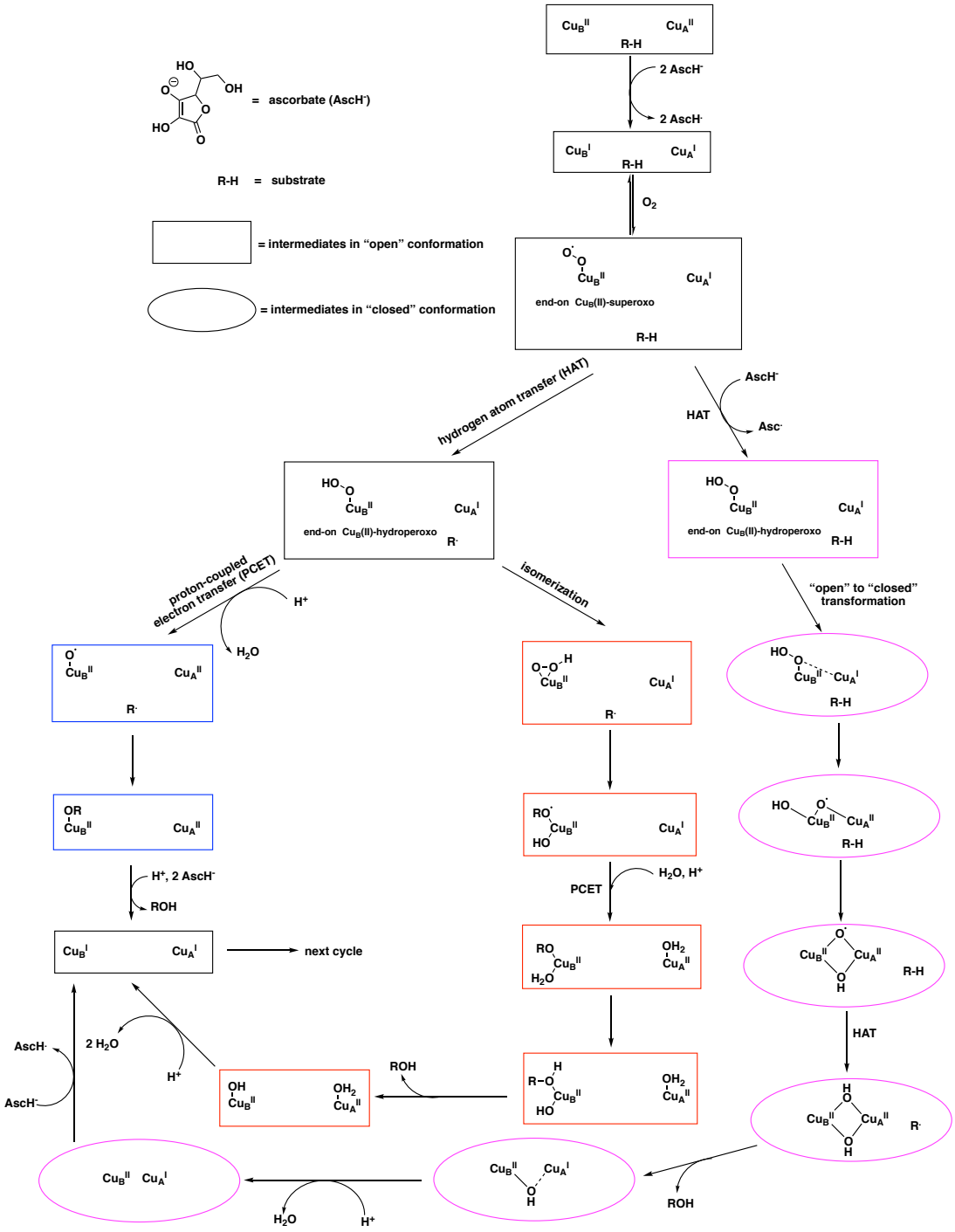

Figure 1-3. Proposed hydroxylation mechanisms for PHM/ DβM. Blue path: Klinman (2006); red path: Cowley et al. (2016); magenta path: Wu et al. (2019). The three pathways, though differ in mechanistic details, agree with each other in terms of forming the end-on Cu_B(II)-superoxo and the end-on Cu_B(II)-hydroperoxo intermediates.

pyramidal geometry coordinating with two ε-histidines, one δ-histidine, and two H_2O molecules at its oxidized resting state (figure 1-5).[10] As the Cu center is reduced, while an X-ray absorption spectroscopic analysis of a few CAO species indicates a decrease of coordination number from five to three, with at least two coordinating histidines, a more recent crystallographic study of *Hansenula polymorpha* amine oxidase 1 (HPAO 1) under limiting O_2 atmosphere suggests a tetrahedral geometry around Cu(I) in a basic environment, which involves the coordination of three histidines and semiquinone (TPQ_{SQ}), the one-electron reduced TPQ after the reductive half-reaction.[1, 10-12]

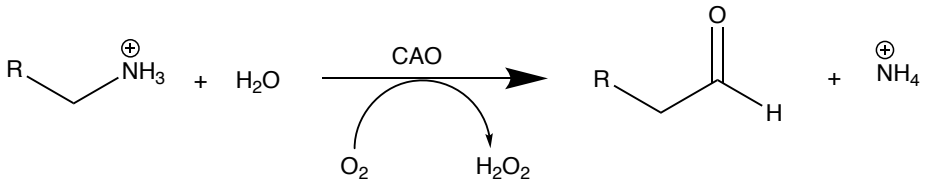

Figure 1-4. Oxidative deamination reaction catalyzed by CAO. In this reaction, O_2 undergoes two-electron reduction to yield H_2O_2, and the amine in the substrate is transformed into an aldehyde. Figure adapted from reference 1.

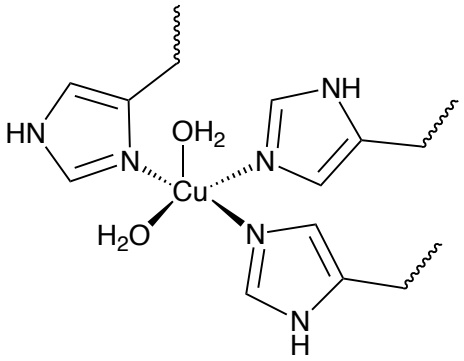

Figure 1-5. The oxidized resting state Cu center in the CAO active site. The Cu center is pentacoordinate with a distorted square pyramidal geometry.[10] Figure adapted from reference 10.

It is generally accepted that CAOs catalyze amine oxidation via a reductive half-reaction followed by an oxidative half-reaction where O_2 is activated (figure 1-6).[10] Disagreements on the

mechanism of the oxidative half-reaction focus mostly on the identity of the one-electron reductant of O_2: it can either be the reduced Cu (figure 1-6 red path) or the two-electron reduced TPQ aminoquinol (TPQ_{AMQ}) (figure 1-6 blue path).[1, 10] CAOs from different sources display distinct propensity toward one of the two possible pathways. While the kinetic data collected for bovine serum amine oxidase (BASO) supports an outer-sphere pathway, those for pea seedling amine oxidase (PSAO), *Arthrobacter globiformis* amine oxidase (AGAO), and *Escherichia coli* amine oxidase (ECAO) support an inner-sphere pathway.[10] Regarding HPAO, although it has been determined based on its metal substitution experiment that it is likely to activate O_2 in an outer-sphere manner, recent detection of a TPQ_{SQ} ligated Cu(I) intermediate in its reaction with limited O_2 suggests a new possibility of O_2 being activated by Cu(I) at an equatorial position and then migrating to an axial position before dissociating as H_2O_2 in a basic environment (figure 1-6 magenta path).[11]

Tripodal-N_4 Mononuclear Cu Complexes as Modelling Systems

The two enzymic systems introduced above are only selected examples of the mononuclear O_2 activating Cu centers in nature. Nevertheless, they clearly show the structural features that are important for modeling such systems using synthetic Cu complexes, as well as the complexity of the possible four-electron and two-electron O_2 reduction mechanisms in Cu-centered metalloenzymes.

The characterizations of the catalytic core in PHM/DβM and CAOs demonstrate the nonplanarity and the richness in histidine coordination around the Cu centers. This is also what makes tripodal-N_4 Cu complexes appropriate modelling systems, because a tripodal-N_4 ligand can easily enforce a nonplanar geometry around the Cu center and mimic the coordinating histidine N atoms (figure 1-7).[13, 14]

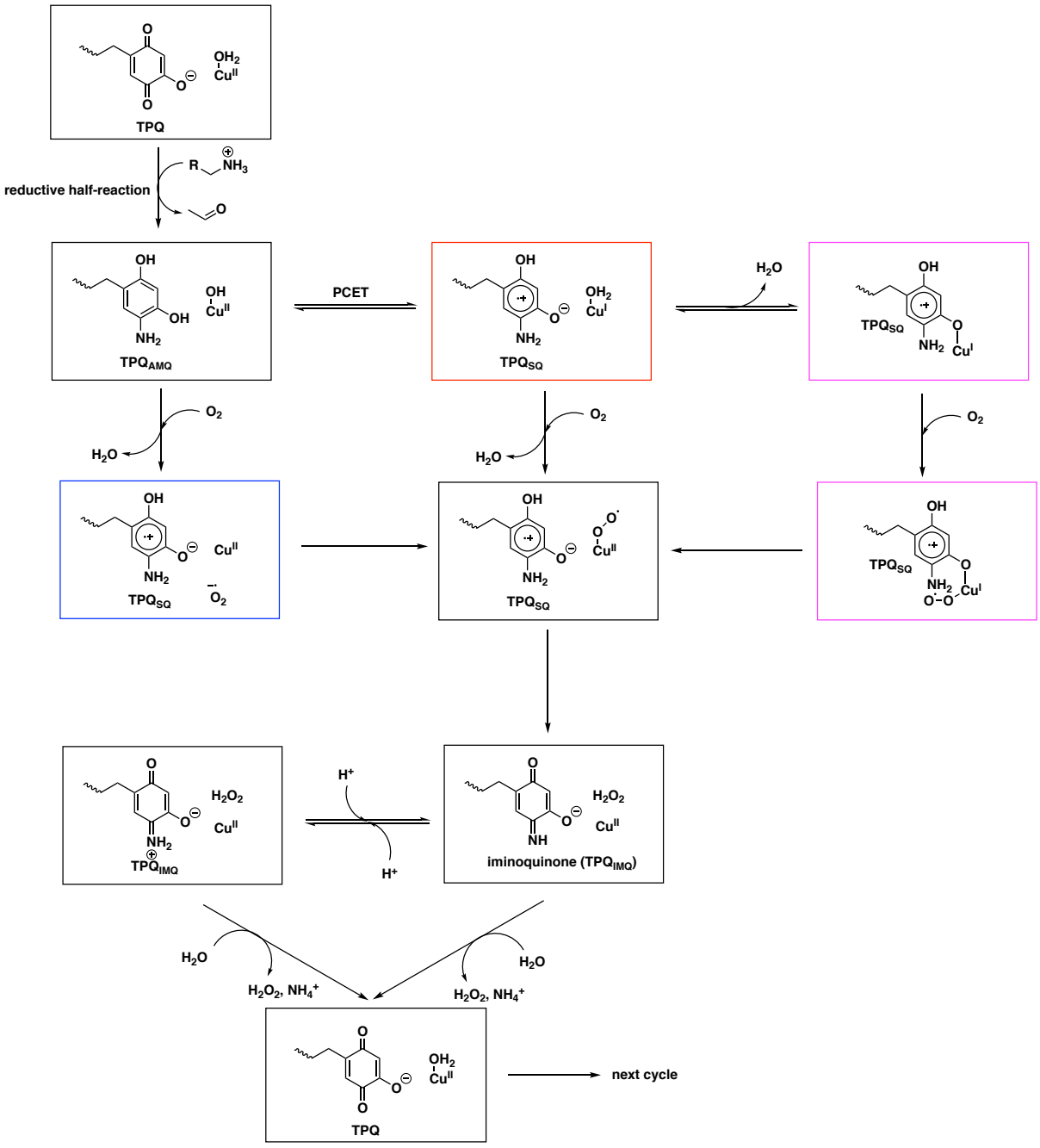

Figure 1-6. Proposed oxidative deamination mechanisms for CAO. The blue box indicates the intermediate found exclusively in the outer-sphere pathway; the red box shows the intermediate found exclusively in the inner-sphere pathway; and the magenta boxes delineate the alternative pathway proposed by Johnson et al. in 2013 for HPAO at pH = 8.5. Black boxes represent intermediates shared by all the pathways.

Many investigations using mononuclear tripodal-N_4 Cu complexes focus on the reaction of a Cu(I) center with O_2, targeting the end-on Cu(II)-superoxo intermediate.[2] At the same time, Cu(II) centered complexes have also been prepared to probe the viable reactive intermediates in the Cu-mediated O_2 activating pathways. These modelling studies have contributed significantly to the elucidation of the working mechanisms of the oxygenases/oxidases in nature and the discovery of novel reactivity which can facilitate the development of new oxidation catalysts.

Tripodal-N_4 Cu(I) Complexes with O_2

The first spectral characterization of a Cu-O_2 adduct was accomplished by Karlin et al. in 1991. In this kinetic study, a Cu(I) complex supported by tris[(2-pyridyl)methyl]amine (tmpa) with a fifth coordinating nitrile molecule was subjected to react with O_2 in propionitirle (figure 1-7).[15] Within the temperature range between $-90℃$ and $-75℃$, the authors observed the rapid formation of $[Cu(tmpa)(O_2)]^+$, characterized by UV-vis absorption peaks (λ_{max}) at 410 nm and 747 nm, which then transformed into $[(Cu(tmpa))_2(O_2)]^{2+}$ bearing a trans-μ-1,2-O_2^{2-} core, characterized by λ_{max} at 525 nm and 590 nm.[15, 16] This allowed the team to propose a mechanism for the reaction between the Cu(I) center and O_2 (figure 1-8).[15] Although many of the tripodal-N_4 Cu complexes synthesized later do not have the fifth coordination of a solvent molecule, this mechanism still finds applicability in those cases.

Many investigations since then have been conducted to establish any structure-function relationship between the tripodal-N_4 ligand backbone of Cu(I) complexes and the formation of their corresponding $[Cu(L)(O_2)]^+$ and/or $[(Cu(L))_2(O_2)]^{2+}$ species. This has generally been done by tuning the geometric, steric, and electronic parameters of the ligands.

Cu(I) complexes supported by bis[(2-pyridyl)methyl]-2-(2-pyridyl)ethylamine (pmea) and bis[2-(2-pyridyl)ethyl]-(2-pyridyl)methylamine (pmap) were synthesized by Schatz et al. and

were both determined to adopt a pseudotetrahedral geometry in the solid state and in acetonitrile (figure 1-7).[17] When both $[Cu(pmea)]^+$ and $[Cu(pmap)]^+$ reacted with O_2 at $-90℃$ in propionitrile, while a transient $[(Cu(pmea))_2(O_2)]^{2+}$ can be detected (λ_{max} at 536 nm), no superoxo or peroxo adducts were observed for $[Cu(pmap)]^+$.[17] The authors attributed this distinction in reactivity to the ability of five-membered chelating rings in stabilizing Cu-oxygen adducts.[17]

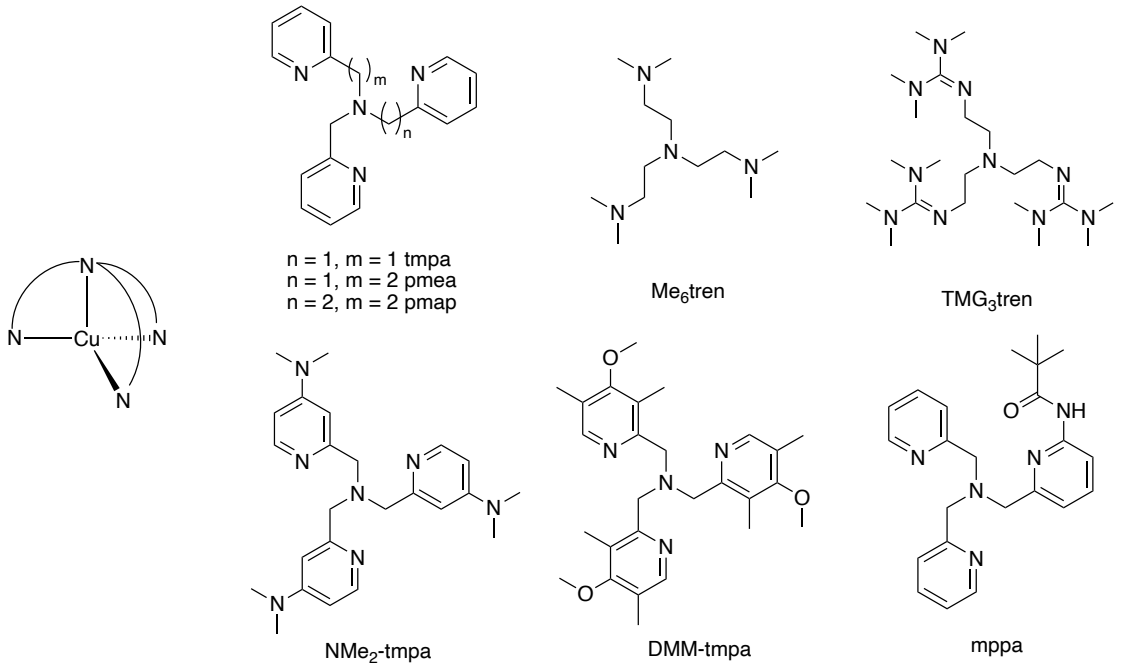

Figure 1-7. Generic structure of a tripodal-N_4 mononuclear Cu complex and reported tripodal-N_4 ligands. The ligand tmpa was used to support a mononuclear Cu complex for the first time in 1982 by Karlin et al. In later studies structural variants of tmpa—pmea and pmap (Schatz et al. 2001), NMe_2-tmpa (Maiti et al. 2007), DMM-tmpa (Lee et al. 2014), and mppa (Peterson et al. 2011)—were employed to elucidate the impact of ligand on the O_2 reactivity of its corresponding tripodal-N_4 Cu(I) complex, as well as the reactivity of the generated Cu-oxygen adducts. Alternative classes of ligands that are based on aliphatic amine—Me_6tren (Becker et al. 1999)—and guanidine—TMG_3tren (Raab et al. 2001)—also contributed to the investigations in this field.

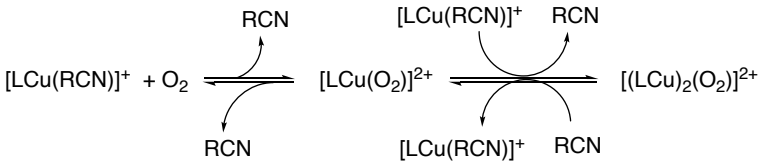

Figure 1-8. Mechanism for Cu(I) reacting with O_2 proposed by Karlin et al. in 1991. Upon the addition of O_2, the Cu complex can exist in equilibrium between a Cu(I) complex, a Cu(II)-superoxo adduct, and a Cu(II)-peroxo dimer species. RCN represents acetonitrile or propionitrile.

A series of studies in the 2000s utilizing tmpa, tris(2-dimethylaminoethyl)amine (Me_6tren), and tris(tetramethylguanidino)tren (TMG_3tren) unveil the roles of basicity and steric hindrance of the tripodal-N_4 ligands in influencing Cu(I) complexes' reactivity with O_2 (figure 1-7). By reacting $[Cu(Me_6tren)(RCN)]^+$ with O_2 in propionitrile in the temperature range between $-90℃$ and $-45℃$, Weitzer et al. detected quick formation of $[Cu(Me_6tren)(O_2)]^+$ (λ_{max} at 412 nm) followed by $[(Cu(Me_6tren))_2(O_2)]^{2+}$ (λ_{max} at 552 nm and 600nm).[18] The measured kinetic and thermodynamic parameters for O_2 reactions with $[Cu(tmpa)(RCN)]^+$ and $[Cu(Me_6tren)(RCN)]^+$ indicate that while $[Cu(Me_6tren)(O_2)]^+$ is more stable than $[Cu(tmpa)(O_2)]^+$, $[(Cu(Me_6tren))_2(O_2)]^{2+}$ is less stable than $[(Cu(tmpa))_2(O_2)]^{2+}$.[18] Considering the fact that Me_6tren is not only more electron-rich but also bulkier than tmpa, the authors argued that while the formation of the superoxo adduct is dominated by the electronic effect, steric hindrance takes precedence in the formation of the peroxo adduct.[18] This finding allowed Würtele et al. to obtain the first crystal structure of a Cu(II)-superoxo species using the TMG_3tren ligand. By incorporating the superbasic, sterically demanding TMG_3tren into a Cu(I) complex, they successfully stabilized $[Cu(TMG_3tren)(O_2)]^+$ and suppressed the formation of $[(Cu(TMG_3tren))_2(O_2)]^{2+}$ at a low temperature, which allowed the collection of $[Cu(TMG_3tren)O_2]SbF_6$ crystals.[19] This crystal structure is the first unambiguous characterization of an end-on Cu(II)-superoxo intermediate supported by a tripodal-N_4 ligand.[19]

The ability to isolate stable $[Cu(L)(O_2)]^+$ species has enabled investigations on their reactivity toward organic substrates. In addition to $[Cu(TMG_3tren)(O_2)]^+$, Cu(II)-superoxo species bearing tris[(4-dimethylamino-2-pyridyl)methyl]amine (NMe_2-tmpa) and tris[(4-methoxy-3,5-dimethylpyridin-2-yl)methyl]amine (DMM-tmpa) ligands were also found to be stable at low temperatures (figure 1-7).[20, 21] All the three species were shown to oxidize 2,6-di-*tert*-butylphenol and its derivatives (*p*-X-DTBP) to 2,6-di-*tert*-butyl-1,4-benzoquinone (DTBQ), likely via an HAT rate-determining step that involves O-H bond homolytic cleavage (figure 1-9).[20-22]

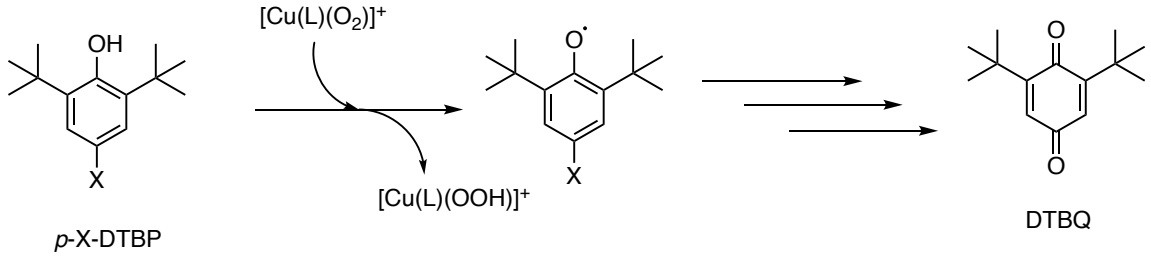

Figure 1-9. Oxidation of *p*-X-DTBP by $[Cu(L)(O_2)]^+$ via HAT. This reaction was found to occur with X = H, OMe, or ^{t}Bu and with L = NMe_2-tmpa, DMM-tmpa, or TMG_3tren. The O-H bond in the phenol substrate was proposed to be cleaved homolytically by a Cu(II)-superoxo adduct $[Cu(L)(O_2)]^+$, which is then transformed into a Cu(II)-hydroperoxo adduct $[Cu(L)(OOH)]^+$.[20]

Regarding C-H bond activation, it has been found that while $[Cu(TMG_3tren)(O_2)]^+$ oxidized *p*-X-DTBP to DTBQ, it also activated a C-H bond on its ligand backbone via the $[Cu(TMG_3tren)(OOH)]^+$ intermediate (figure 1-10).[22] The first intermolecular C-H activation was realized by the Cu(II)-superoxo adduct supported by bis(pyrid-2-ylmethyl)[(6-(pivalamido) pyrid-2-yl)methyl)amine] (mppa) (figure 1-7).[23, 24] At $-125℃$, $[Cu(mppa)(O_2)]^+$ activated a C-H bond in 1-benzyl-1,4-dihydronicotinamide (BNAH) (figure 1-11).[23] Kinetic studies show that this reaction also occurred via a rate-limiting HAT with C-H homolytic cleavage.[23]

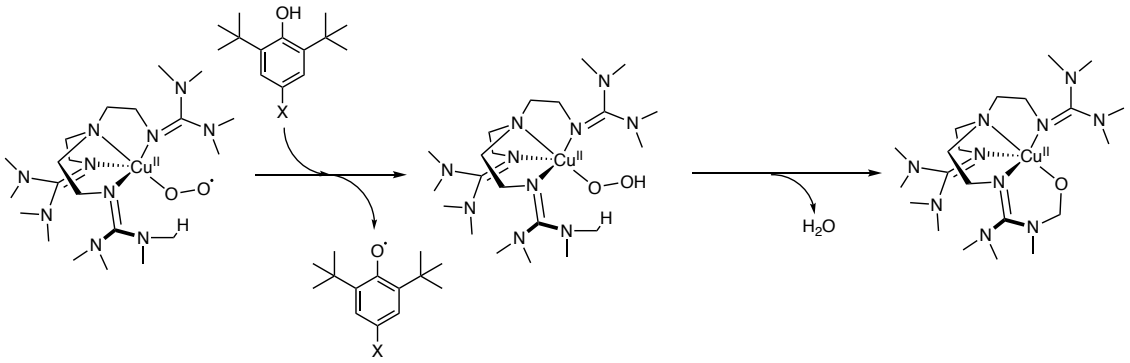

Figure 1-10. Intramolecular C-H activation in $[Cu(TMG_3tren)(O_2)]^+$. After abstracting a hydrogen atom from the phenol substrate, $[Cu(TMG_3tren)(O_2)]^+$ transforms into $[Cu(TMG_3tren)(OOH)]^+$, which then undergoes a homolytic O-O bond cleavage and activates a (sp^3)C-H bond on the ligand backbone along with the production of H_2O.[22] Figure adapted from reference 22.

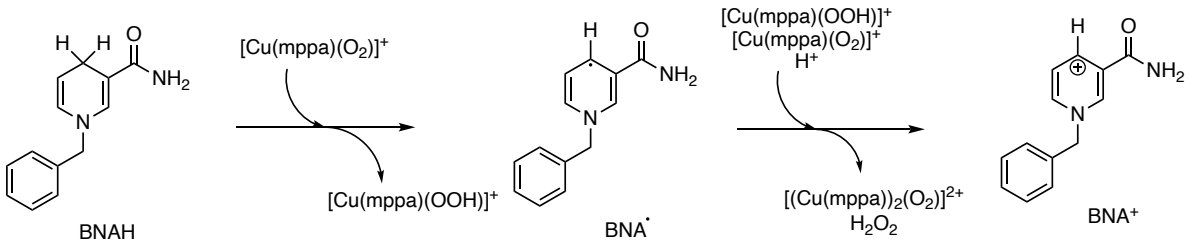

Figure 1-11. Intermolecular C-H Activation in BNAH mediated by $[Cu(mppa)(O_2)]^+$. $[Cu(mppa)(O_2)]^+$ activates a (sp^3)C-H bond in the substrate (BNAH) and yields $[Cu(mppa)(OOH)]^+$ along with the substrate radical ($BNA^{\bullet}$), which can be further oxidized by the Cu(II)-superoxo and hydroperoxo adducts to form a cation (BNA^+) with H_2O_2 and a Cu(II)-peroxo dimer species as byproducts.[23]

Preparation of Tripodal-N_4 Cu(II) Complexes in Predicting the Oxidized Intermediates

In several studies where the reaction between tripodal-N_4 Cu(I) complexes and O_2 was investigated, their Cu(II) counterparts were also prepared and characterized.[14, 17, 25-27] In most cases, no further investigations were conducted on these Cu(II) complexes. However, these

Cu(II) complexes can serve the purpose of predicting the geometry of the Cu(I) complex after it reacts with O_2. For example, the initial proposal that end-on $[Cu(tmpa)(O_2)]^+$ was an intermediate for the oxidation of $[Cu(tmpa)]^+$ to $[(Cu(tmpa))_2(O_2)]^+$ was primarily based on the trigonal bipyramidal geometry of $[Cu(tmpa)(Cl)]^+$.[14, 15, 28] However, caution should be taken when applying this approach, as the geometry of the corresponding Cu(II) complexes only suggests a possibility. In the 2001 study conducted my Schatz et al., while the authors failed to detect any superoxo or peroxo species for $[Cu(pmap)]^+$, they synthesized $[Cu(pmap)(Cl)]^+$ easily.[17]

In addition to structural prediction, in a few cases the Cu(II) complex was reacted with selected oxidants to support the intermediacy of certain structures on the pathway of the reactions between a Cu(I) complex and O_2. A prominent example for such applications is related to the intramolecular C-H activation reaction in figure 1-10. An important piece of evidence for the involvement of $[Cu(TMG_3tren)(OOH)]^+$ in the oxygenation reaction was that treating the corresponding Cu(II) complex $[Cu(TMG_3tren)]^{2+}$ with deprotonated H_2O_2 yielded exactly the same product as in the superoxo mediated condition.[22]

As the Cu(II)-hydroperoxo species has been shown to be an active intermediate in many superoxo mediated reactions, reacting Cu(II) complexes directly with H_2O_2 has become an alternative method for facilitating oxidation reactions. In 2020, Muthuramalingam et al. successfully employed a series of pyridine/amine based tripodal-N_4 Cu(II) complexes as catalysts for benzene hydroxylation.[29] A Cu(II)-hydroperoxo reactive intermediate was implicated spectrally and computationally.

Reference

1. Peterson, R. L.; Kim, S.; Karlin, K. D., 3.07 - Copper Enzymes. In *Comprehensive Inorganic Chemistry II (Second Edition)*, Reedijk, J.; Poeppelmeier, K., Eds. Elsevier: Amsterdam, 2013; pp 149-177.

2. Elwell, C. E.; Gagnon, N. L.; Neisen, B. D.; Dhar, D.; Spaeth, A. D.; Yee, G. M.; Tolman, W. B., Copper–Oxygen Complexes Revisited: Structures, Spectroscopy, and Reactivity. *Chemical Reviews* **2017,** *117* (3), 2059-2107.

3. Klinman, J. P., The Copper-Enzyme Family of Dopamine β-Monooxygenase and Peptidylglycine α-Hydroxylating Monooxygenase: Resolving the Chemical Pathway for Substrate Hydroxylation*. *Journal of Biological Chemistry* **2006,** *281* (6), 3013-3016.

4. Prigge, S. T.; Kolhekar, A. S.; Eipper, B. A.; Mains, R. E.; Amzel, L. M., Amidation of Bioactive Peptides: The Structure of Peptidylglycine α-Hydroxylating Monooxygenase. *Science* **1997,** *278* (5341), 1300-1305.

5. Prigge, S. T.; Kolhekar, A. S.; Eipper, B. A.; Mains, R. E.; Amzel, L. M., Substrate-mediated electron transfer in peptidylglycine α-hydroxylating monooxygenase. *Nature Structural Biology* **1999,** *6* (10), 976-983.

6. Prigge, S. T.; Eipper, B. A.; Mains, R. E.; Amzel, L. M., Dioxygen Binds End-On to Mononuclear Copper in a Precatalytic Enzyme Complex. *Science* **2004,** *304* (5672), 864-867.

7. Wu, P.; Fan, F.; Song, J.; Peng, W.; Liu, J.; Li, C.; Cao, Z.; Wang, B., Theory Demonstrated a “Coupled” Mechanism for O2 Activation and Substrate Hydroxylation by Binuclear Copper Monooxygenases. *Journal of the American Chemical Society* **2019,** *141* (50), 19776-19789.

8. Cowley, R. E.; Tian, L.; Solomon, E. I., Mechanism of O2 activation and substrate hydroxylation in noncoupled binuclear copper monooxygenases. *Proceedings of the National Academy of Sciences* **2016,** *113* (43), 12035.

9. Vendelboe, T. V.; Harris, P.; Zhao, Y.; Walter, T. S.; Harlos, K.; El Omari, K.; Christensen, H. E. M., The crystal structure of human dopamine β-hydroxylase at 2.9 Å resolution. *Science advances* **2016,** *2* (4), e1500980-e1500980.

10. Shepard, E. M.; Dooley, D. M., Inhibition and Oxygen Activation in Copper Amine Oxidases. *Accounts of Chemical Research* **2015,** *48* (5), 1218-1226.

11. Johnson, B. J.; Yukl, E. T.; Klema, V. J.; Klinman, J. P.; Wilmot, C. M., Structural Snapshots from the Oxidative Half-reaction of a Copper Amine Oxidase: IMPLICATIONS FOR O2 ACTIVATION*. *Journal of Biological Chemistry* **2013,** *288* (39), 28409-28417.

12. Dooley, D. M.; Scott, R. A.; Knowles, P. F.; Colangelo, C. M.; McGuirl, M. A.; Brown, D. E., Structures of the Cu(I) and Cu(II) Forms of Amine Oxidases from X-ray Absorption Spectroscopy. *Journal of the American Chemical Society* **1998,** *120* (11), 2599-2605.

13. Karlin, K. D.; Hayes, J. C.; Hutchinson, J. P.; Hyde, J. R.; Zubieta, J., Synthesis and x-ray structural characterization of Cu(I) and Cu(II) derivatives of a new symmetric tripodal ligand N(CH2CH2-py)3, (py = 2-pyridyl). *Inorganica Chimica Acta* **1982,** *64*, L219-L220.

14. Karlin, K. D.; Hayes, J. C.; Juen, S.; Hutchinson, J. P.; Zubieta, J., Tetragonal vs. trigonal coordination in copper(II) complexes with tripod ligands: structures and properties of [Cu(C21H24N4)Cl]PF6 and [Cu(C18H18N4)Cl]PF6. *Inorganic Chemistry* **1982,** *21* (11), 4106-4108.

15. Karlin, K. D.; Wei, N.; Jung, B.; Kaderli, S.; Zuberbuehler, A. D., Kinetic, thermodynamic, and spectral characterization of the primary copper-oxygen (Cu-O2) adduct in a

reversibly formed and structurally characterized peroxo-dicopper(II) complex. *Journal of the American Chemical Society* **1991,** *113* (15), 5868-5870.

16. Jacobson, R. R.; Tyeklar, Z.; Farooq, A.; Karlin, K. D.; Liu, S.; Zubieta, J., A copper-oxygen (Cu2-O2) complex. Crystal structure and characterization of a reversible dioxygen binding system. *Journal of the American Chemical Society* **1988,** *110* (11), 3690-3692.

17. Schatz, M.; Becker, M.; Thaler, F.; Hampel, F.; Schindler, S.; Jacobson, R. R.; Tyeklár, Z.; Murthy, N. N.; Ghosh, P.; Chen, Q.; Zubieta, J.; Karlin, K. D., Copper(I) Complexes, Copper(I)/O2 Reactivity, and Copper(II) Complex Adducts, with a Series of Tetradentate Tripyridylalkylamine Tripodal Ligands. *Inorganic Chemistry* **2001,** *40* (10), 2312-2322.

18. Weitzer, M.; Schindler, S.; Brehm, G.; Schneider, S.; Hörmann, E.; Jung, B.; Kaderli, S.; Zuberbühler, A. D., Reversible Binding of Dioxygen by the Copper(I) Complex with Tris(2-dimethylaminoethyl)amine (Me6tren) Ligand. *Inorganic Chemistry* **2003,** *42* (6), 1800-1806.

19. Würtele, C.; Gaoutchenova, E.; Harms, K.; Holthausen, M. C.; Sundermeyer, J.; Schindler, S., Crystallographic Characterization of a Synthetic 1:1 End-On Copper Dioxygen Adduct Complex. *Angewandte Chemie International Edition* **2006,** *45* (23), 3867-3869.

20. Lee, J. Y.; Peterson, R. L.; Ohkubo, K.; Garcia-Bosch, I.; Himes, R. A.; Woertink, J.; Moore, C. D.; Solomon, E. I.; Fukuzumi, S.; Karlin, K. D., Mechanistic insights into the oxidation of substituted phenols via hydrogen atom abstraction by a cupric-superoxo complex. *Journal of the American Chemical Society* **2014,** *136* (28), 9925-9937.

21. Maiti, D.; Fry, H. C.; Woertink, J. S.; Vance, M. A.; Solomon, E. I.; Karlin, K. D., A 1:1 Copper−Dioxygen Adduct is an End-on Bound Superoxo Copper(II) Complex which

Undergoes Oxygenation Reactions with Phenols. *Journal of the American Chemical Society* **2007,** *129* (2), 264-265.

22. Maiti, D.; Lee, D.-H.; Gaoutchenova, K.; Würtele, C.; Holthausen, M. C.; Narducci Sarjeant, A. A.; Sundermeyer, J.; Schindler, S.; Karlin, K. D., Reactions of a Copper(II) Superoxo Complex Lead to C-H and O-H Substrate Oxygenation: Modeling Copper-Monooxygenase C-H Hydroxylation. *Angewandte Chemie International Edition* **2008,** *47* (1), 82-85.

23. Peterson, R. L.; Himes, R. A.; Kotani, H.; Suenobu, T.; Tian, L.; Siegler, M. A.; Solomon, E. I.; Fukuzumi, S.; Karlin, K. D., Cupric superoxo-mediated intermolecular C-H activation chemistry. *Journal of the American Chemical Society* **2011,** *133* (6), 1702-1705.

24. Yamaguchi, S.; Wada, A.; Funahashi, Y.; Nagatomo, S.; Kitagawa, T.; Jitsukawa, K.; Masuda, H., Thermal Stability and Absorption Spectroscopic Behavior of (μ-Peroxo)dicopper Complexes Regulated with Intramolecular Hydrogen Bonding Interactions. *European Journal of Inorganic Chemistry* **2003,** *2003* (24), 4378-4386.

25. Raab, V.; Kipke, J.; Burghaus, O.; Sundermeyer, J., Copper Complexes of Novel Superbasic Peralkylguanidine Derivatives of Tris(2-aminoethyl)amine as Constraint Geometry Ligands. *Inorganic Chemistry* **2001,** *40* (27), 6964-6971.

26. Will, J.; Würtele, C.; Becker, J.; Walter, O.; Schindler, S., Synthesis, crystal structures and reactivity towards dioxygen of copper(I) complexes with tripodal aliphatic amine ligands. *Polyhedron* **2019,** *171*, 448-454.

27. Paria, S.; Morimoto, Y.; Ohta, T.; Okabe, S.; Sugimoto, H.; Ogura, T.; Itoh, S., Copper(I)–Dioxygen Reactivity in the Isolated Cavity of a Nanoscale Molecular Architecture. *European Journal of Inorganic Chemistry* **2018,** *2018* (19), 1976-1983.

28. Schatz, M.; Raab, V.; Foxon, S. P.; Brehm, G.; Schneider, S.; Reiher, M.; Holthausen, M. C.; Sundermeyer, J.; Schindler, S., Combined Spectroscopic and Theoretical Evidence for a Persistent End-On Copper Superoxo Complex. *Angewandte Chemie International Edition* **2004,** *43* (33), 4360-4363.

29. Muthuramalingam, S.; Anandababu, K.; Velusamy, M.; Mayilmurugan, R., Benzene Hydroxylation by Bioinspired Copper(II) Complexes: Coordination Geometry versus Reactivity. *Inorganic Chemistry* **2020,** *59* (9), 5918-5928.

Chapter 2. Synthesis, Characterization, and Preliminary Reactivity Study of Two Novel Cu Complexes with a Tripodal Amidate Ligand

Introduction

Although numerous mononuclear Cu complexes that are supported by a wide variety of tripodal-N_4 ligands have already been investigated, all these reported ligands are neutral. With the hope to further expand the scope of tripodal-N_4 Cu complexes available as potential oxidation catalysts, a few questions were proposed at the beginning of the current study:

- Is it possible to prepare a tripodal-N_4 Cu complex supported by a charged ligand?
- How would a charged ligand influence the structural features of a tripodal-N_4 Cu complex?
- How would a charged ligand affect the oxidative reactivity of a tripodal-N_4 Cu complex, specifically the O_2 reactivity of a tripodal-N_4 Cu(I) complex? Would such a ligand backbone enable any new reactivity?

With an aim to address these questions, in this study an anionic amidate ligand 2, 2‘, 2‘‘-tris(trifluoroamido)triphenylamine (N(*o*-PhNHC(O)CF_3)$_3$) was incorporated to a redox pair of Cu complexes, (PPh_4)$_2$[Cu(N(*o*-PhNC(O)CF_3)$_3$)] (**1**) and PPh_4[Cu(N(*o*-PhNC(O)CF_3)$_3$)] (**2**) (scheme 2-1; scheme 2-2). Both **1** and **2** were successfully synthesized with yields above 65%. Their unusual structures were characterized via single-crystal X-ray crystallography and several other spectral and electrochemical techniques.

The preliminary reactivity study of **1** with O_2 did not yield the expected pattern corresponding to a Cu(II)-superoxo and/or Cu(II)-peroxo adduct, and the reaction pathway cannot be definitively described based on the collected data. Nonetheless, during the

coordinating reaction between **1** and Et_4NCN, an unexpected O-atom transfer reaction was discovered. Besides, a novel ligand hydroxylation product was isolated in the preparation of **2**.

Synthesis and Characterization of Complex 1 and 2

Synthesis of the Ligand and the Metal Complexes

The synthesis of the N(*o*-PhNHC(O)CF_3)$_3$ (**H_3L^{CF3}**) ligand was based on modified published procedures (scheme 2-1). First, tris(2-nitrophenyl)amine (N(*o*-$PhNO_2$)$_3$) was prepared via an aromatic nucleophilic substitution reaction between commercially available 2-nitroaniline and 1-fluoro-2-nitrobenzene.[1] Then, N(*o*-$PhNO_2$)$_3$ was converted to tris(2-aminophenyl)amine (N(*o*-$PhNH_2$)$_3$) through hydrogenation catalyzed by 5% Pd/C.[1] Finally, the target **H_3L^{CF3}** ligand was produced through a nucleophilic acyl substitution reaction between N(*o*-$PhNH_2$)$_3$ and trifluoroacetic anhydride.[2]

Scheme 2-1. Synthesis of the N(*o*-PhNHC(O)CF_3)$_3$ Ligand

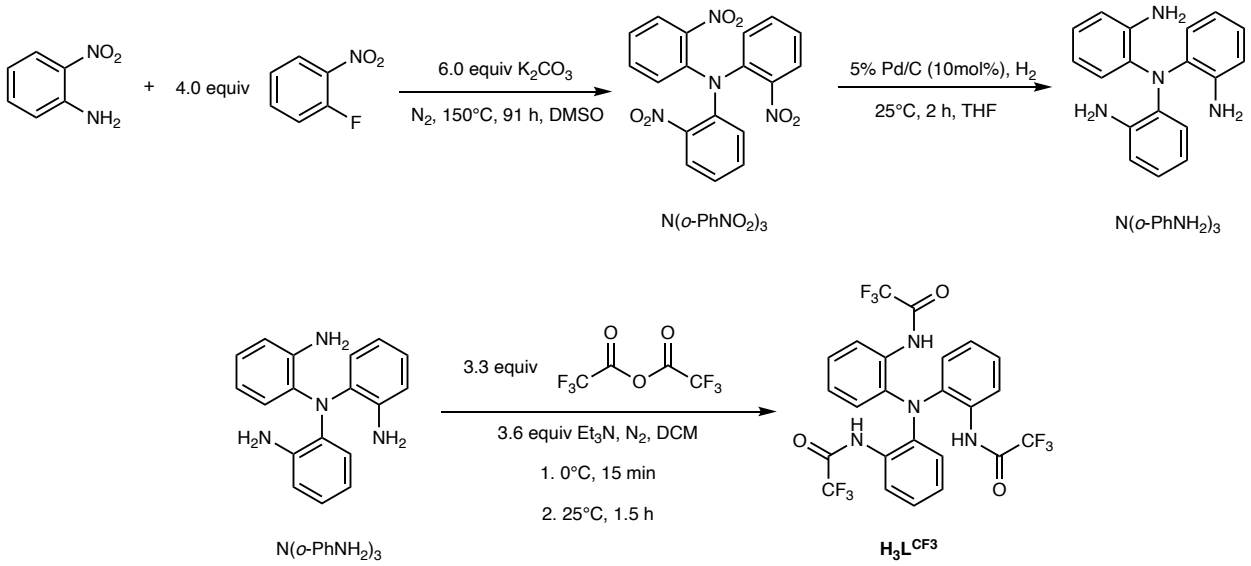

The syntheses of **1** and **2** required the addition of three equivalent of potassium hydride to completely deprotonate the ligand first. Then, one equivalent of the corresponding Cu bromide salt was added for metalation. Finally, after the salt metathesis step with the addition of

tetraphenylphosphonium bromide, **1** and **2** were produced (Scheme 2-2). The only byproduct of both syntheses was potassium bromide, which was easily removed by redissolving the reaction mixture in acetonitrile and doing a filtration. Upon the optimization of the reaction condition and work-up procedures, the yields of **1** and **2** were raised to 70% and 82%, respectively.

Scheme 2-2. Syntheses of Complex 1 and 2

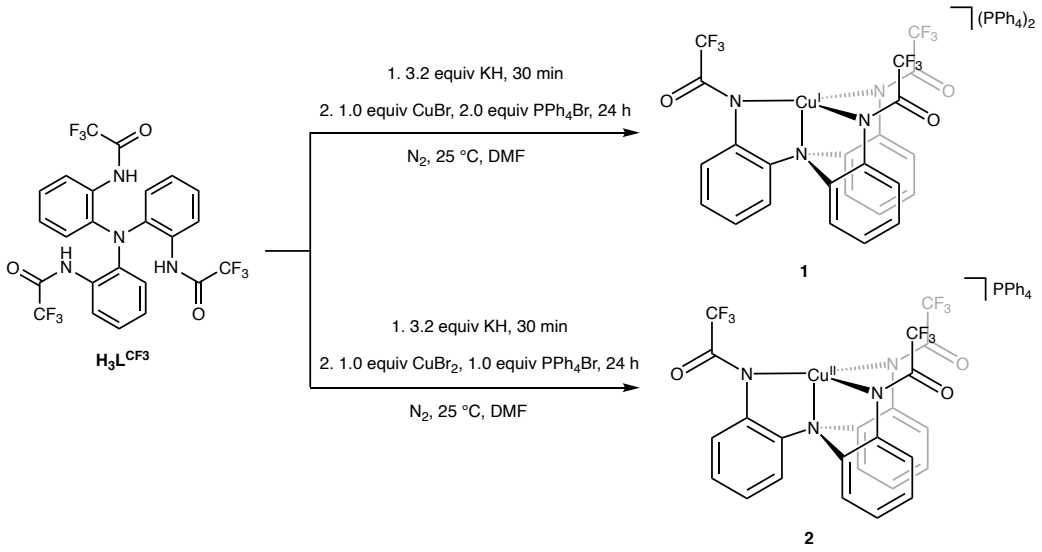

*Solid-state Molecular Structures of **1** and **2***

X-ray diffraction quality crystal of **1**, an orange solid, was obtained through vapor diffusion of diethyl ether into a concentrated solution of **1** in acetonitrile, and that of **2**, a dark purple solid, was obtained through layer diffusion of hexane into a concentrated solution of **2** in dichloromethane. The solid-state molecular structure of both **1** and **2** show the coordination between the Cu center with the N atoms on the deprotonated $\mathbf{H_3L^{CF3}}$ ligand ($\mathbf{[L^{CF3}]}^{3-}$) (figure 2-1). The N_{ap}-Cu-N_{eq} angles in the two complexes are all smaller than 90° (table 2-1).

The solid-state structure of **1** does not show the fifth coordination of the acetonitrile molecule to the Cu center, which differentiates it from $[Cu(tmpa)]^{+}$.[3] Notably, the Cu-N4 bond in **1** is significantly longer than those in many of the previously reported four-coordinate Cu(I)

complexes supported by a neutral tripodal-N_4 ligand.[4-11] This is possibly due to the labiling effect caused by the three negatively-charged amidate N atoms: the high electron density donated by the equatorial N atoms to the Cu center significantly weakens its interaction with the apical N atom.

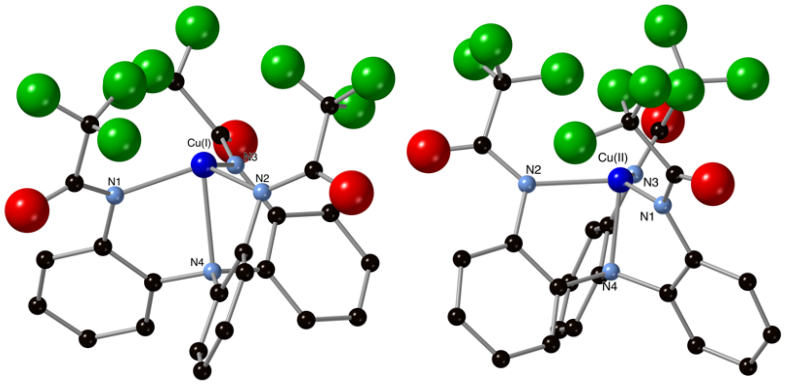

Figure 2-1. Solid-state molecular structures of **1** (left) and **2** (right). Hydrogen atoms and the countercation PPh_4^+ are omitted for clarity.

Table 2-1. Selected Bond Lengths (Å) and Angles (°) for Complex 1 and 2

	1	**2**[a]
Cu-N1	2.052	1.901
Cu-N2	2.031	2.085
Cu-N3	2.021	1.934
Cu-N4	2.359	2.059
N1-Cu1-N2	113.33	108.40
N1-Cu1-N3	115.97	140.50
N1-Cu1-N4	77.50	84.42
N2-Cu1-N3	118.23	107.79
N2-Cu1-N4	78.66	83.07
N3-Cu1-N4	78.06	83.77

[a] Bond lengths and angles are averaged over two independent Cu(II) complexes in one asymmetric unit for **2**.

Although almost all the reported tripodal-N_4 supported Cu(II) complexes are five-coordinate, interestingly, **2** does not have the fifth coordinating ligand, which makes its structure quite unusual.[3, 4, 6, 11, 12] However, after a careful examination of the crystallographic data of **2**, it was identified that the distance between one of the nine fluorine atoms on the ligand backbone and the Cu center is only around 2.4 Å. This interatomic distance is not short enough to be considered as representing a Cu-F bond, which should be close to 2.0 Å based on reported data.[6, 13-16] Nonetheless, it is indicative of a weak interaction between the F atom on the ligand and the Cu(II) center. The existence of this additional interaction is reminiscent of the reported five-coordinate geometry of tripodal-N_4 Cu(II) complexes, and this can explain why another ligand does not coordinate.

*Characterization of **1** and **2** in Solution*

The sharp chemical shifts in the ^{1}H NMR spectrum of **1** in deuterated acetonitrile indicate that it is closed shell d^{10} diamagnetic and that the coordination of the solvent molecule to the Cu center did not occur. Evidence in support of a tetracoordinate geometry of complex **1** in solution also include the almost identical UV-vis and ^{1}H NMR behavior of **1** observed in acetonitrile, a coordinating solvent, and in dichloromethane, a non-coordinating solvent (figure 2-2; figure 2-3).

The cyclic voltammogram of **1**, however, shows distinct features in acetonitrile and in dichloromethane (figure 2-4). When a scan rate of 100mV/s was applied, while an electrochemically complex profile was observed for **1** in acetonitrile, only one irreversible oxidation event was observed for **1** in dichloromethane. It is worth noting that as the scan rate was raised to 500mV/s and 1000mV/s, the electrochemical profiles of **1** in the two solvents become more similar. At this point, a robust argument cannot yet be made to explain this solvent-dependent difference in electrochemistry. One possibility is that the additional

electrochemical events for **1** in acetonitrile result from trace amounts of impurities in the solvent, which were quickly consumed. This postulation can be supported by the observation that there are fewer electrochemical events in the third sweep than in the first sweep in the 100mV/s acetonitrile scan of **1** (figure 2-4 (a)). One way to test this hypothesis is to repeat the experiment using newly purified acetonitrile as the solvent. If a similar pattern as in figure 2-4 (a) is still seen, then it might be helpful to use spectral techniques such as UV-Vis and ^{1}H NMR to characterize the species obtained after each sweep of the cyclic voltammetry scan of **1** in both acetonitrile and dichloromethane to identify any differences, since there are no significant distinctions in **1**'s behavior in the two solvents when it is undisturbed. The irreversible nature of the oxidation event of **1**, which can be seen clearly in figure 2-4 (b)-(d), is supported by its diminishing with increasing scan rates. Furthermore, this event is consistent with a mechanism where an irreversible homogeneous chemical reaction occurs after a reversible electron transfer.[17]

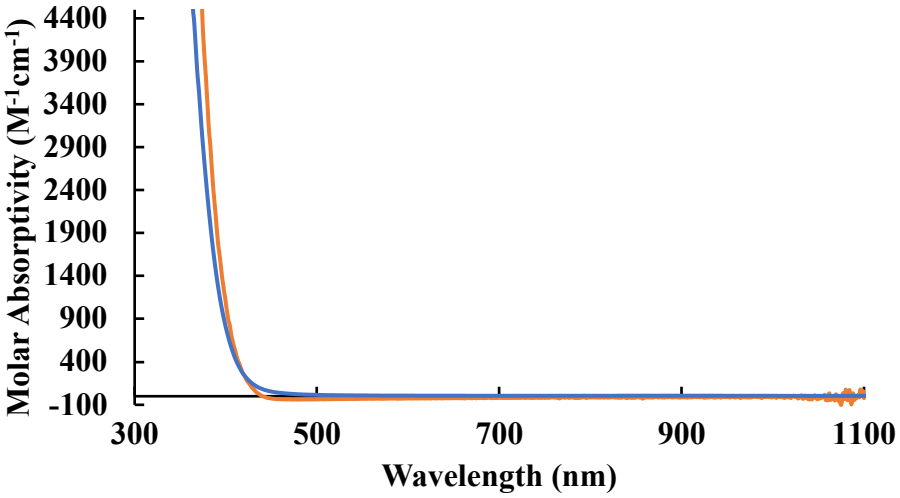

Figure 2-2. The UV-vis spectrum of **1** in acetonitrile (orange trace) and in dichloromethane (blue trace) at 25℃. In neither of the two solvents does **1** display any absorption peaks.

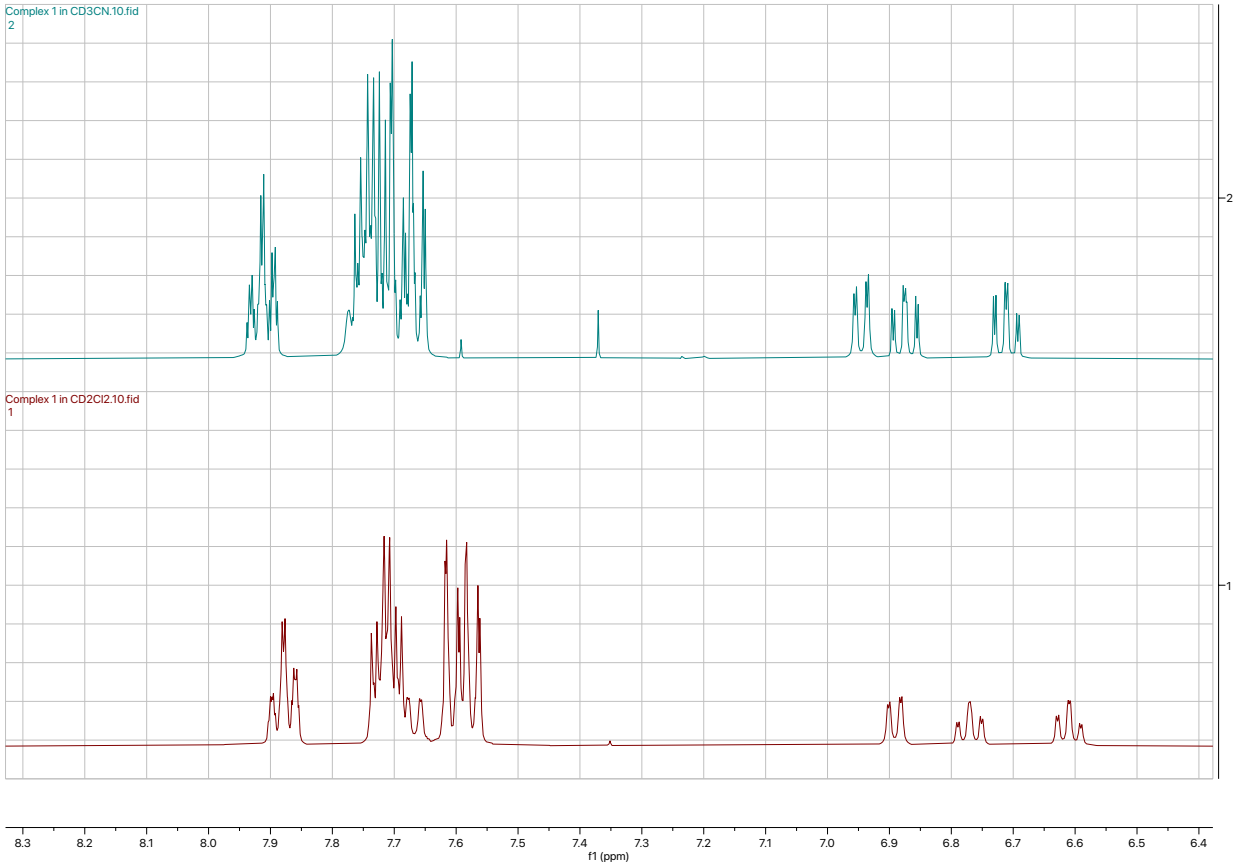

Figure 2-3. The ^{1}H NMR spectrum of **1** in deuterated acetonitrile (top) and dichloromethane (bottom). In both solvents, chemical shifts signifying PPh_4^+ (δ 7.91 td in acetonitrile and δ 7.94-7.84 m in dichloromethane) and three groups of aromatic protons (δ 6.95 dd, δ 6.90-6.85 m, δ 6.71 td in acetonitrile and δ 6.89 dd, δ 6.82-6.73 m, δ 6.61 td in dichloromethane) can be clearly seen. Peak integrations in both solvents (see experimental section) agree with the asymmetric unit structure of **1** shown in scheme 2-2.

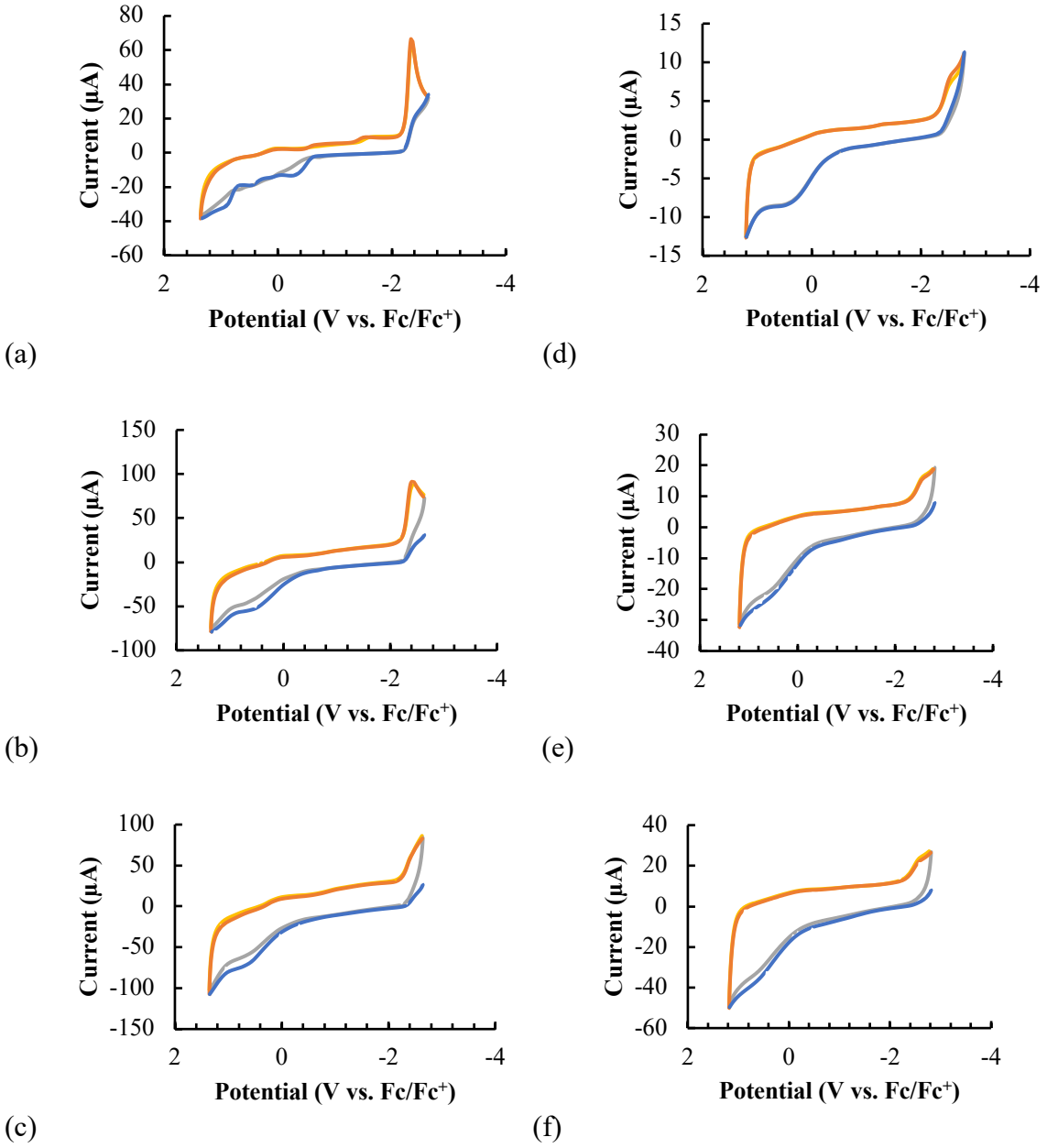

Figure 2-4. Cyclic voltammogram of 1.0mM **1** with 0.1 M $TBAPF_6$ as supporting electrolyte at 25℃. (a)-(c): cyclic voltammogram of **1** in acetonitrile with a scan rate of 100mV/s, 500mV/s, and 1000mV/s, respectively. (d)-(f): cyclic voltammogram of **1** in dichloromethane with a scan rate of 100mV/s, 500mV/s, and 1000mV/s, respectively. In each of the six voltammograms, blue trace is the first sweep, orange trace is the second sweep, grey trace is the third sweep, and yellow trace is the fourth sweep.

In contrast to **1**, complex **2** displays more complicated behaviors in solution. In the ^{1}H NMR spectrum of **2** in both deuterated acetonitrile and dichloromethane, inexplicable diamagnetic signals were observed in addition to the broadened peaks that result from the d^9 paramagnetic Cu(II) center (figure 2-5; figure 2-6). Although the difference in ^{1}H NMR behavior of **2** in the two solvents may suggest a disruption of the structure of **2** which results from the coordination of acetonitrile molecules to the Cu(II) center, the convoluted signals in the range of 6.5-7.5 ppm observed in deuterated dichloromethane imply the influence of other factors as well. Since the ^{1}H NMR data is generally not reported for paramagnetic tripodal-N_4 Cu(II) complexes in literature, comparisons with precedent cases cannot be easily made. While it may seem reasonable to argue that one/more of the coordination interactions between the Cu center and $\mathbf{[L^{CF3}]^{3-}}$ could become loose in solution and thus result in structural rearrangement of **2** or even a polymerization, past studies in which such a phenomenon was observed tend to involve a coordinating solvent like acetonitrile or a proton source like water, which were all absent in the ^{1}H NMR sample of **2** in deuterated dichloromethane in this case.[18-21] One way to further explore the dynamics of **2** in dichloromethane is through subjecting **2** to each of the solvents that were present in the current ^{1}H NMR sample—hexane, diethyl ether, dimethylformamide, toluene, and dichloromethane itself—and monitoring any change in the ^{1}H NMR pattern.

Due to the ambiguity of the structure of **2** in solution as revealed by its ^{1}H NMR spectra, systematic characterization of this species in acetonitrile and dichloromethane was not further carried out using cyclic voltammetry and UV-vis spectroscopy.

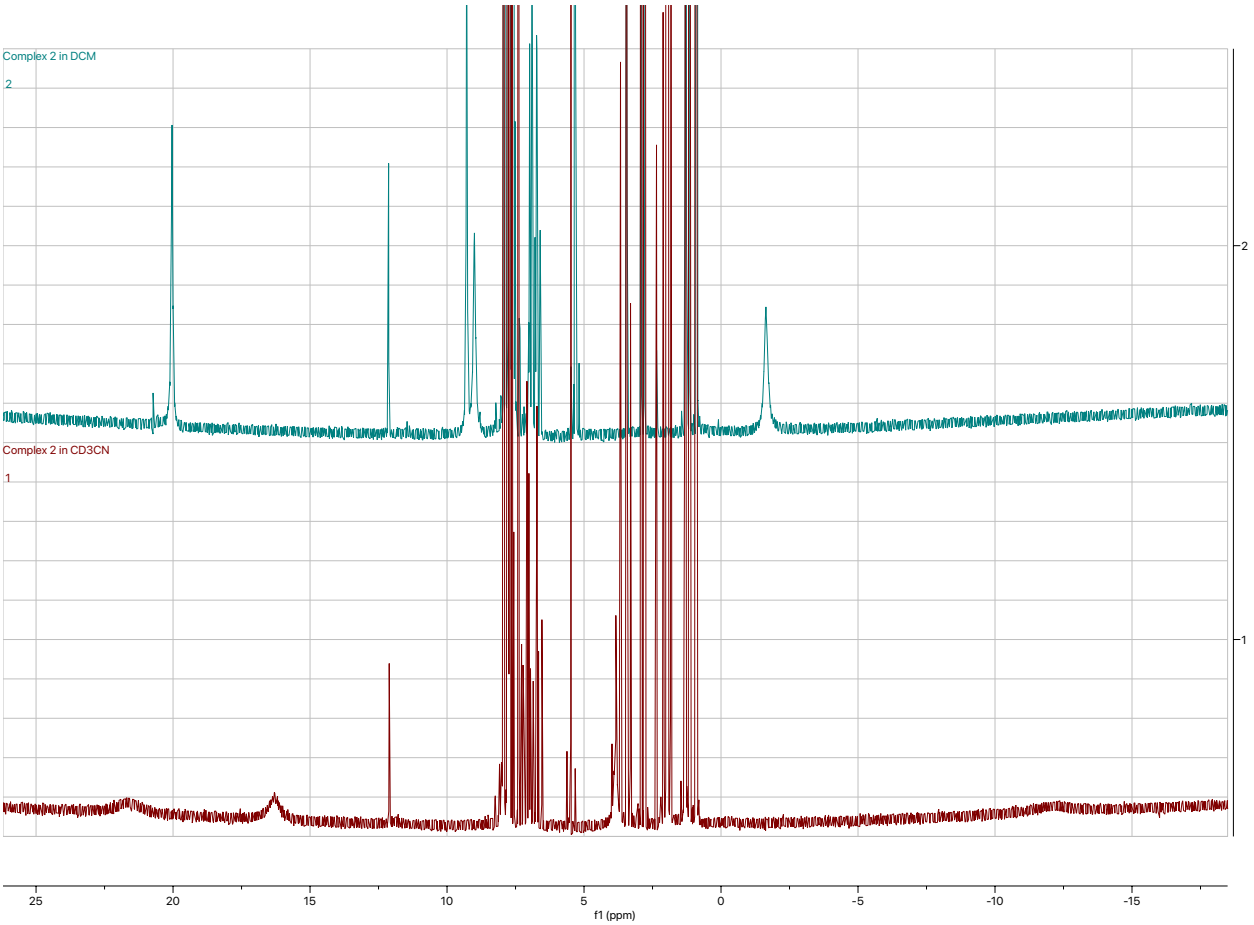

Figure 2-5. The ^{1}H NMR spectrum of **2** in deuterated dichloromethane (top) and acetonitrile (bottom). Paramagnetic peaks can be identified at δ 20.02, 9.27, 8.99, -1.65 for **2** in deuterated dichloromethane, and at δ 21.52, 16.26, -12.10 for **2** in deuterated acetonitrile.

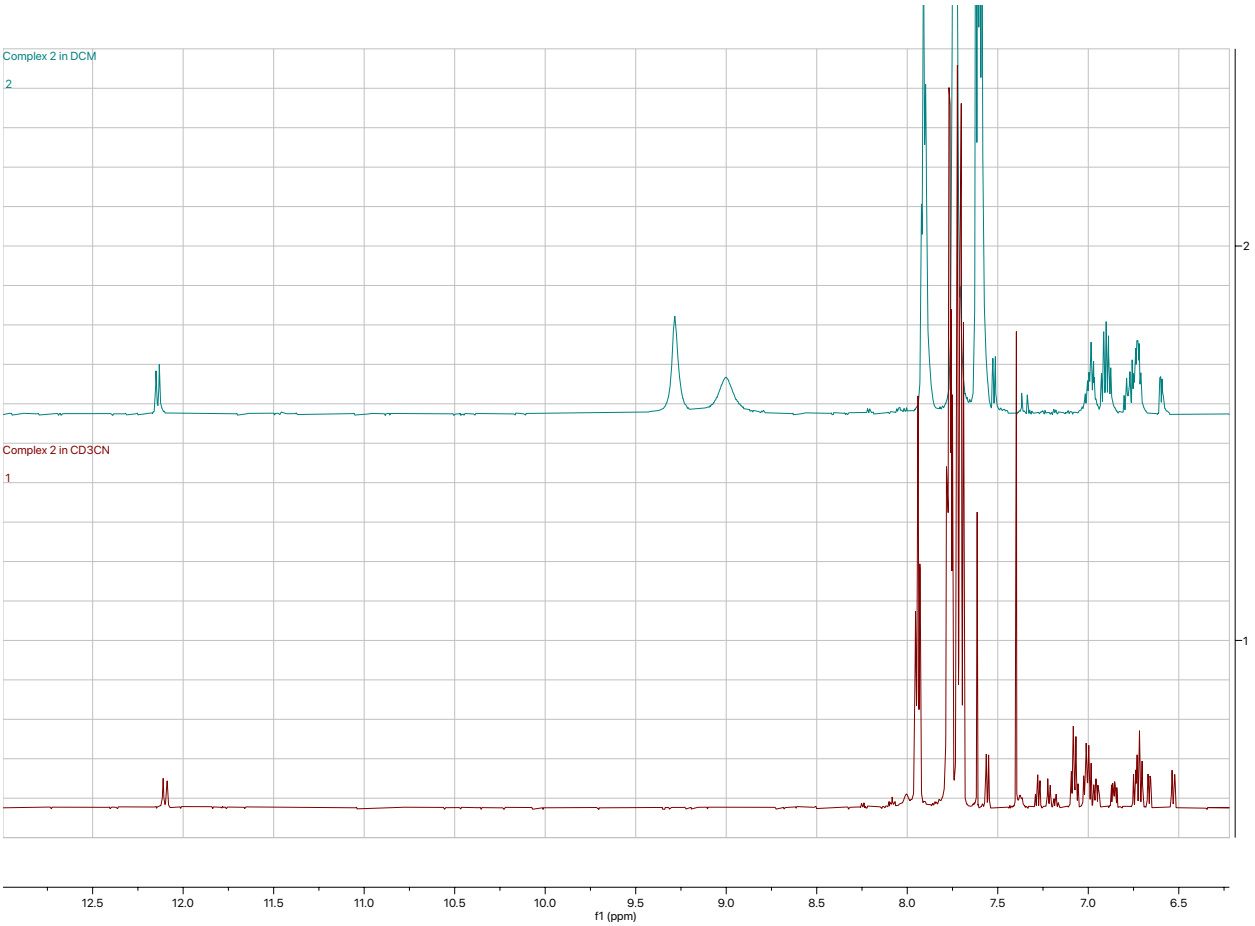

Figure 2-6. The amplified ^{1}H NMR spectrum of **2** in deuterated dichloromethane (top) and acetonitrile (bottom). In both solvents, convoluted diamagnetic chemical shifts were observed in 6.5-7.5 ppm.

Preliminary Oxidative Reactivity Studies of Complex 1 and 2

*Reaction of Complex **1** with O_2 at Room Temperature*

Once **1** was fully characterized, its reactivity toward O_2 was investigated. A preliminary evaluation of the O_2 reactivity of **1** at room temperature in acetonitrile shows a slow emergence of peaks at 585 nm and 800 nm, followed by a shoulder at 465 nm. The presence of one isosbestic point suggests the transformation of **1** into a different species (figure 2-7).

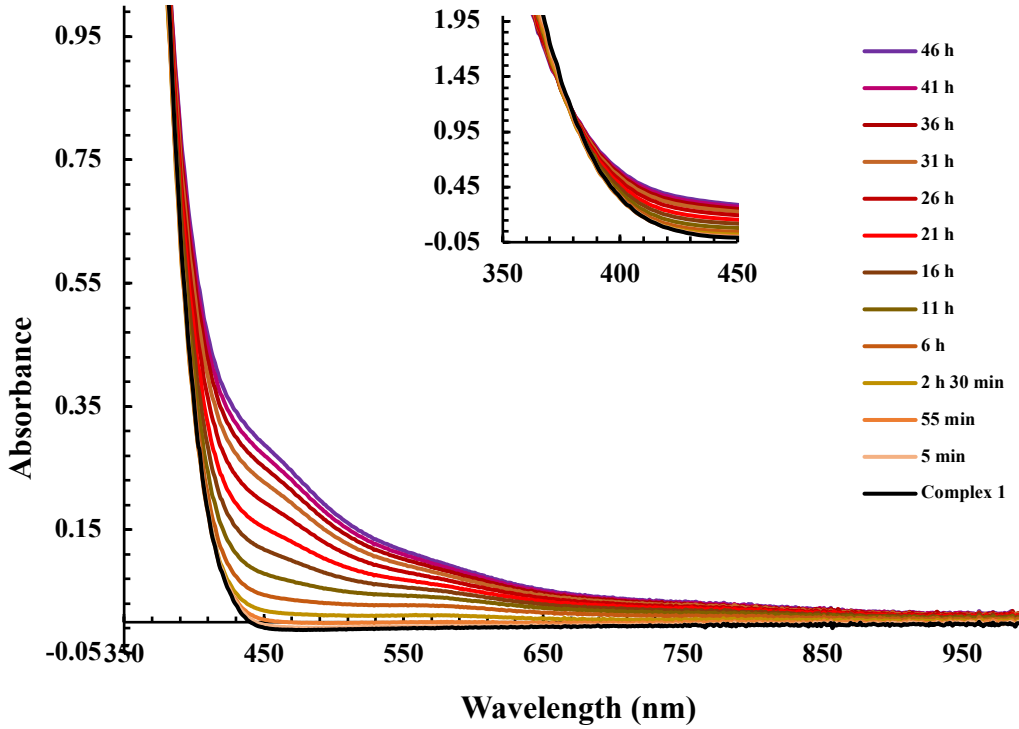

Figure 2-7. The UV-vis spectrum of **1** (0.33mM) in acetonitrile upon addition of excess dioxygen at 25℃. The insert shows the isosbestic point.

The observed UV-vis pattern is not consistent with the characteristic ligand-metal charge transfer (LMCT) bands corresponding to a $[Cu(L)(O_2)]^+$ or $[(Cu(L))_2(O_2)]^{2+}$ adduct, which are expected to locate at 400-450 nm and 500-550 nm, respectively.[11, 20, 22-27] Furthermore, the reaction of **1** with O_2 was sluggish, compared to many precedent cases where the Cu(I) complex of a similar concentration reacted with O_2 fairly rapidly at much lower temperatures to yield the UV-vis patterns for $[Cu(L)(O_2)]^+$ or $[(Cu(L))_2(O_2)]^{2+}$.[5, 6, 11, 20, 27] For this reason, the reaction of **1** with O_2 was not monitored at a lower temperature.

The sensitivity to temperature of the reaction between a Cu(I) complex and O_2 has been discussed in a few studies, and the authors have suggested the pathways of decomposition of $[(Cu(L))_2(O_2)]^{2+}$ or $[Cu(L)(O_2)]^+$ as temperature is raised.[6, 18, 23, 27] However, while it may be tempting to surmise that the UV-vis pattern in figure 2-7 can also represent the decomposed

species following the instant formation of Cu(II)-superoxo or Cu(II)-peroxo adducts, there is not enough evidence to support this postulate, since in previous studies the spectroscopic characterizations of the decomposed species were generally not reported. To decipher the UV-vis absorption features in figure 2-7, one viable way would be monitoring the reaction between **1** and O_2 at a lower temperature, which can be realized by using liquid nitrogen, with UV-vis spectroscopy. If the LMCT bands corresponding to $[Cu(L)(O_2)]^+$ and/or $[(Cu(L))_2(O_2)]^{2+}$ are observed, and these bands gradually decay to the pattern seen in figure 2-7 as temperature increases to 25℃, the decomposition postulate will be supported. Alternatively, if almost no spectral change can be observed, then this will be the evidence for **1**'s inertness toward O_2.

A few studies also proposed the reaction outcome that the Cu(I) complex was "slowly oxidized" to its Cu(II) counterpart without the coordination of O atom(s) to the Cu center.[20, 28] To examine whether this pathway is applicable to the scenario in figure 2-7, a UV-vis spectrum of **2** in acetonitrile was taken (figure 2-8). For **2** in acetonitrile at room temperature, broad peaks at 586 nm and 803 nm, as well as a shoulder near 400 nm can be observed. These features do resemble those seen in the reaction between **1** and O_2 to some extent (figure 2-7). Thus, the possibility that **1** was slowly oxidized to **2** under an O_2 atmosphere at room temperature cannot be excluded, although solid evidence for this mechanism would require isolating diffraction-quality crystals from the reaction mixture, which has so far been unsuccessful.

In addition to the pathways discussed above in which the electron transfer occurs between the Cu(I) center and O_2, since $\mathbf{H_3L^{CF3}}$ belongs to a family of redox-active ligands, an outer-sphere mechanism should also be considered. In fact, while the cyclic voltammetry of **1** shows an irreversible oxidative event, whether this event is associated with the Cu center or with the ligand is unknown. Therefore, it would be valuable to also measure the electrochemistry of $\mathbf{H_3L^{CF3}}$ in

acetonitrile at room temperature so that a more comprehensive understanding of the redox properties of **1** can be generated.

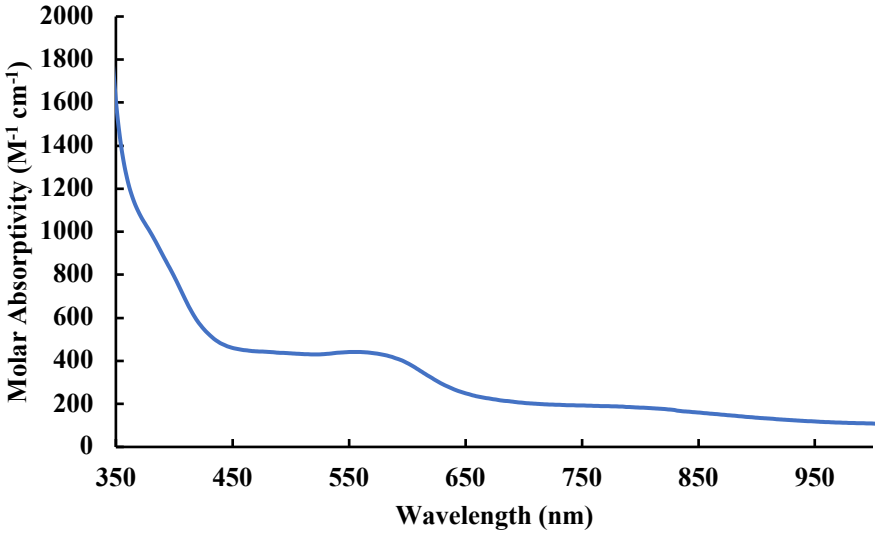

Figure 2-8. The UV-vis spectrum of **2** in acetonitrile at 25℃. The concentration of **2** was determined based on its solid-state structure.

*Countercation Oxidation in Complex **1** in Presence of Tetraethylammonium Cyanide (Et_4NCN)*

While working up the coordination reaction between **1** and Et_4NCN in drybox, the crystals of triphenylphosphine oxide ($P(O)Ph_3$) were isolated (scheme 2-3). This was quite unexpected due to the involvement of the countercation PPh_4^+, and the source of the O atom in the $P(O)Ph_3$ product was also perplexing. Previous research has indicated that the transformation of PPh_4^+ to $P(O)Ph_3$ would require an O-nucleophile, which is absent in reaction scheme 2-3 since the carbonyl O atom in $\mathbf{[L^{CF3}]^{3-}}$ is highly electrophilic and cyanide is not expected to attack amide.[29] Therefore, possible external O atom sources were considered, and it was suspected that trace amounts of O_2 in the drybox may interfere with this reaction.

Scheme 2-3. Reaction of 1 with Et_4NCN in Drybox

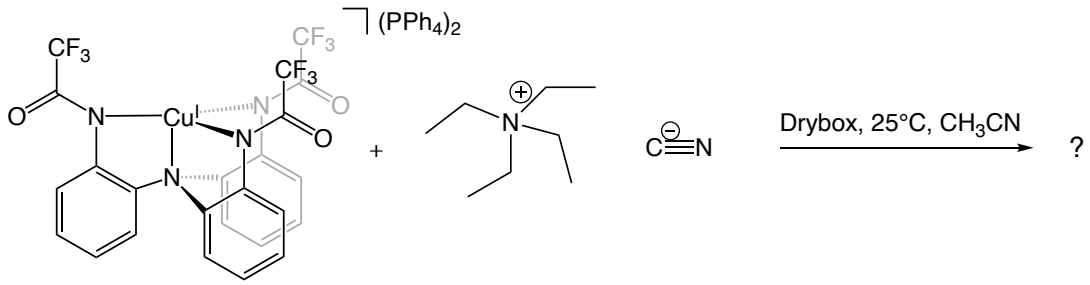

Therefore, the reaction of **1** with Et_4NCN was tracked using ^{31}P NMR both when conducted in the drybox and with the addition of excess O_2. In all the ^{31}P NMR spectra obtained only the chemical shift of PPh_4^+ at δ 22.91 and/or that of $P(O)Ph_3$ at δ 25.95 can be observed. By calculating the ratio of the peak integrations of the two species at different time points, a preliminary kinetic curve was plotted for the two reaction conditions (figure 2-9). The graph shows that as O_2 was introduced, there was a significant acceleration of the formation of $P(O)Ph_3$. This supports a positive role played by O_2 in this reaction.

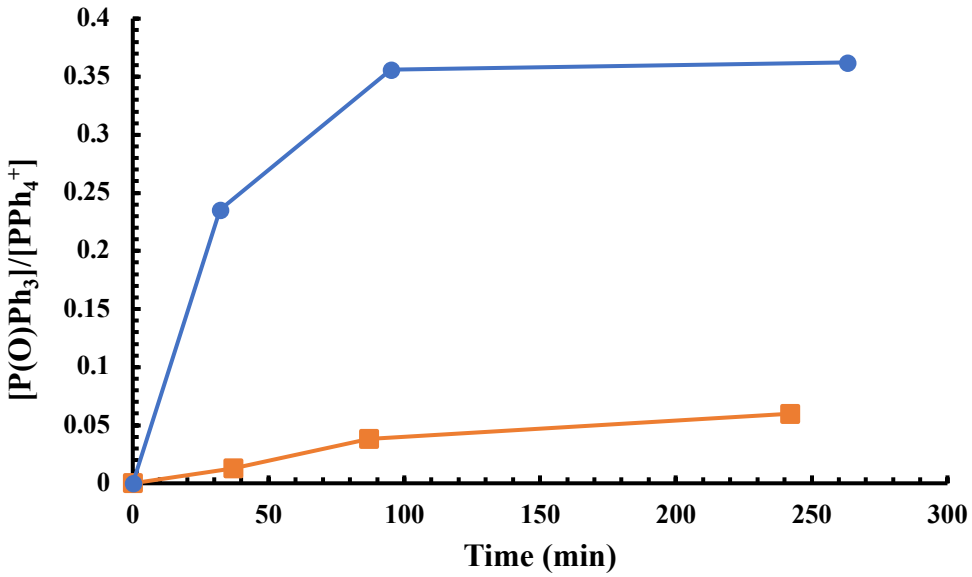

Figure 2-9. Formation of $P(O)Ph_3$ in the reaction between **1** and Et_4NCN in acetonitrile at 25°C in drybox (orange trace) and under an O_2 atmosphere (blue trace).

To elucidate the mechanism of this reaction, a control experiment was done where an acetonitrile solution of **1** was exposed to excess O_2 without adding Et_4NCN. In this scenario, no formation of the $P(O)Ph_3$ product was detected. This observation indicates the important role of Et_4NCN in the oxygenation of PPh_4^+. Notably, a weak IR peak at 2109 cm^{-1} was detected in the mixture of the reaction shown in scheme 2-3 (figure 2-10), which is consistent with the μ_2-CN coordination mode in a binuclear Cu complex bearing the tmpa ligand at 2107 cm^{-1} (figure 2-11).[30] Thus, it is worth trying to prepare a similar structure as $[Cu_2(tmpa)_2CN]^+$ using the $\mathbf{[Cu(L^{CF3})]^{2-}}$ species ($\mathbf{[1]^{2-}}$) in the current study and test whether $[Cu_2(L^{CF3})_2CN]^+$ is capable of mediating the O-atom transfer from O_2 to a PPh_4^+ salt in acetonitrile. The result of this experiment would provide important clues for the mechanistic pathways of the formation of $P(O)Ph_3$ in the current case.

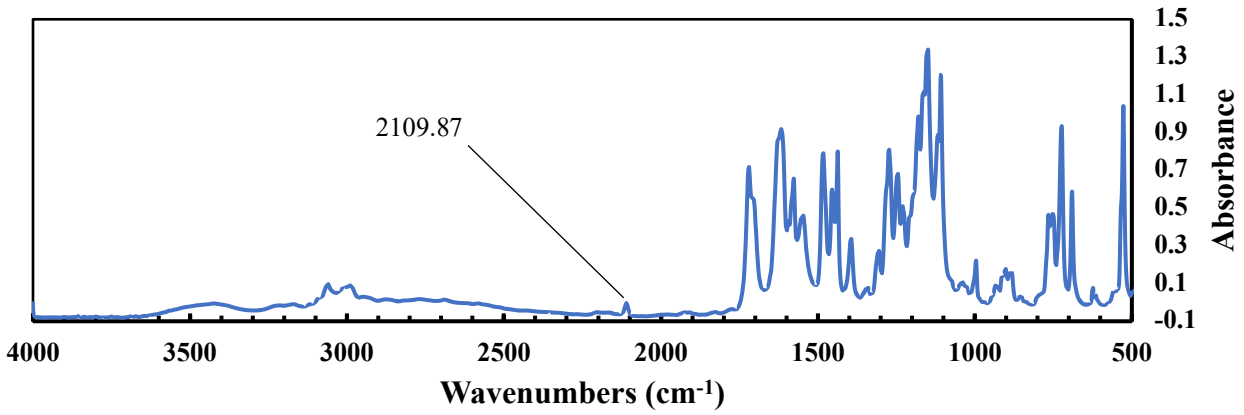

Figure 2-10. Infrared spectrum of the dried reaction mixture of **1** with Et_4NCN in acetonitrile at 25℃ in drybox. A weak peak at 2109 cm^{-1} was detected, which falls in the energy range of Cu-cyanide coordination interactions.

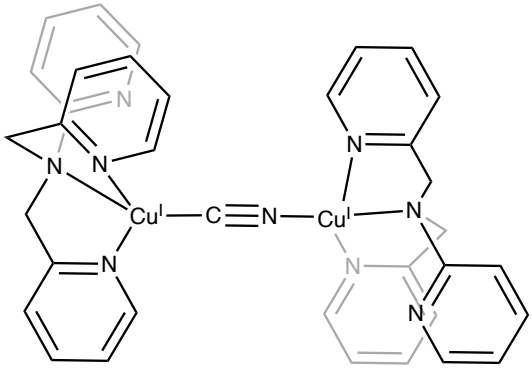

Figure 2-11. Structure of $[Cu_2(tmpa)_2CN]^+$. In its solid state the complex shows a tridentate coordination mode at each Cu(I) center with one of the pyridyl groups of tmpa uncoordinated.[30] Figure adapted from reference 30.

As the preparation of $[Cu_2(tmpa)_2CN]^+$ also involves the mixing of Et_4NCN and the Cu(I) complex precursor, it would be helpful to switch to a less reactive countercation for $\mathbf{[1]^{2-}}$. An attempt to synthesize $\mathbf{[1]^{2-}}(Et_4N)_2$ (**1'**) shows promise in this approach, as diffraction-quality crystals were successfully isolated through vapor diffusion of diethyl ether into concentrated acetonitrile solution of **1'** (scheme 2-4). The solid-state structure of **1'** has a perfect C_3 symmetry along its Cu-N_{ap} axis, and the structural parameters of **1'** highly resemble those of **1** (figure 2-12). The yield of **1'**, however, needs to be further improved, and other potential choices of countercations—such as NMe_4^+, $N(n\text{-}Bu)_4^+$, imidazolium—should also be considered since they tend to yield more ordered crystals.

Scheme 2-4. Synthesis of Complex 1'

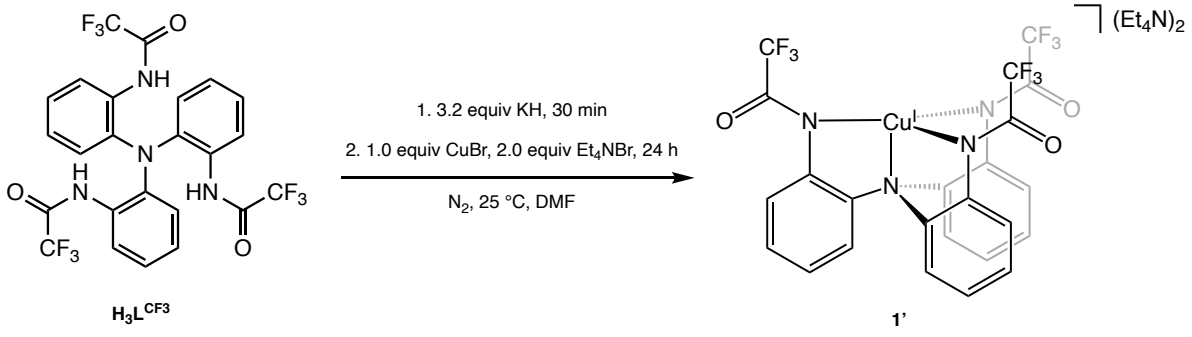

H_3L^{CF3} 1'

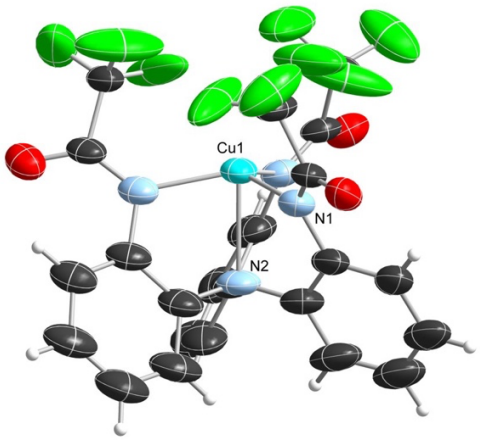

Figure 2-12. Solid-state molecular structure of **1'**. The countercation Et_4N^+ is omitted for clarity. Cu-N1: 2.057 Å, Cu-N2: 2.288 Å; N1-Cu-N1: 116.80°, N1-Cu-N2: 79.58°.

A caveat for the series of ^{31}P NMR kinetic experiments, however, is the generation of a small amount of white precipitate for the reaction of **1** with Et_4NCN both in drybox and under O_2 atmosphere. This precipitate intriguingly has a poor solubility in many common solvents spanning a wide range of polarity, including water, methanol, dimethyl sulfoxide, chloroform, acetonitrile, benzene, and hexane. Therefore, its identity cannot be determined and the only characterization of it is its solid-state IR spectrum which shows a sharp peak at 2118 cm^{-1}, likely corresponding to a different Cu-cyanide coordination mode that does not have a precedent in literature (figure 2-13). In all the ^{31}P NMR experiments, an internal standard was not used in case it would react. As a result, the progress of the formation of $P(O)Ph_3$ from PPh_4^+ presented in figure 2-9 was calculated based on an assumption that the white precipitate, which cannot be detected by ^{31}P NMR, does not contain any P element. Considering this limitation, a more meticulous way to track the source of O atom in $P(O)Ph_3$ should be carrying out the same reaction under $^{18}O_2$ and detecting any isotopic incorporation in the product using mass spectrometry. Although a preliminary trial shows that the regular electrospray ionization (ESI)

mass spectrometry fails to detect an intact $P(O)Ph_3$ molecule, other ionization methods such as atmospheric pressure chemical ionization (APCI) are worth trying.

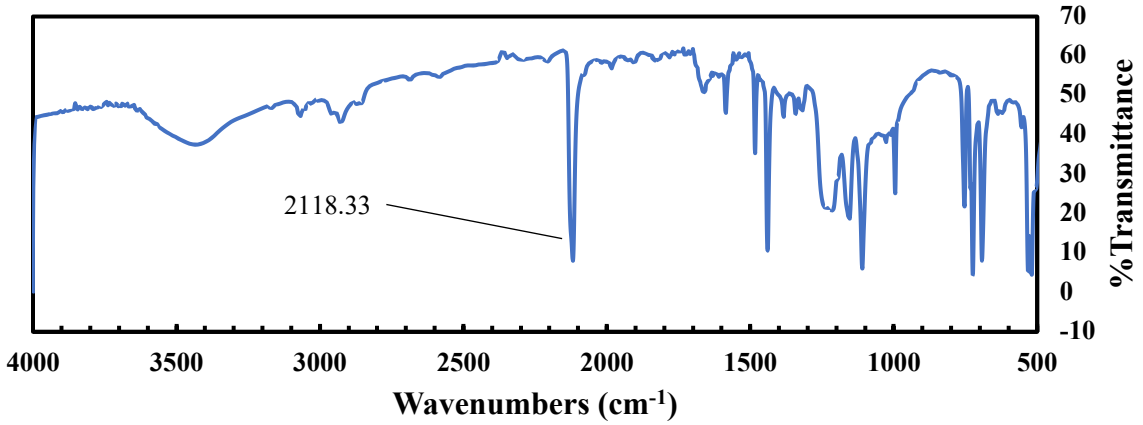

Figure 2-13. Infrared spectrum of the white precipitate in the reaction mixture of **1** with Et_4NCN in acetonitrile at 25℃ in drybox. A sharp peak at 2118 cm^{-1} was observed, which falls in the energy range of Cu-cyanide coordination interactions.

*Observation of a C-F Bond Hydroxylation in Preparation of Complex **2***

While optimizing the synthesis of complex **2**, in one trial it was observed that 1/3 of the product underwent hydroxylation of one of the nine C-F bonds on its ligand backbone. This new complex (**3**) co-crystallized with **2** upon layer diffusion of hexane into a concentrated dichloromethane solution of the product (figure 2-14).

The distance between the O atom in the hydroxyl group and the Cu center is 2.405 Å. Similar to the solid-state characterization of **2**, although such a distance is too long to be considered as a Cu-O bond, it suggests a significant interaction between the Cu(II) center and the O atom.[31-33] This is reflected by the overall longer bond lengths between Cu and the four N atoms, and the Cu-N_{ap} bond was lengthened to the greatest extent (table 2-2).

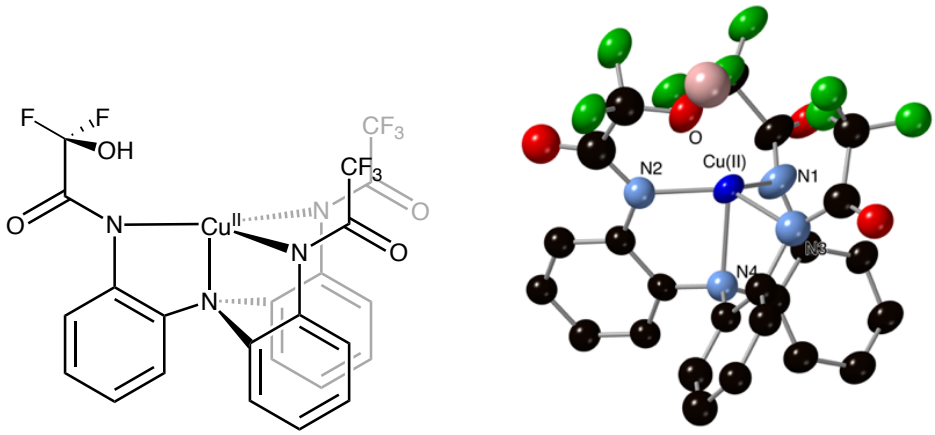

Figure 2-14. Molecular structure of **3**. Aromatic hydrogens and the countercation PPh_4^+ are omitted for clarity.

Table 2-2. Bond Lengths (Å) and Angles (°) for Complex 3

Bond Length (Å)		Bond Angle (°)	
Cu-N1	2.179	N1-Cu-N4	77.49
Cu-N4	2.201	N1-Cu-N2	113.87
Cu-N3	2.049	N1-Cu-N3	105.02
Cu-N2	1.898	N3-Cu-N4	82.97
		N2-Cu-N4	82.52
		N3-Cu-N2	134.06

Hydroxylation of a sp^3 C-F bond is not a commonly seen reaction, and one representative example from literature is the catalytic pathway of nonheme iron 2-oxoglutarate dependent oxygenases, although strictly speaking hydroxylation is not the endpoint of this reaction (figure 2-15).[34] In this mechanism, an oxoiron(IV) intermediate is involved and a C-H bond homolytic cleavage has to occur. On the contrary, only activation of an aromatic C-F bond has been reported for Cu-dioxygen adducts.[35]

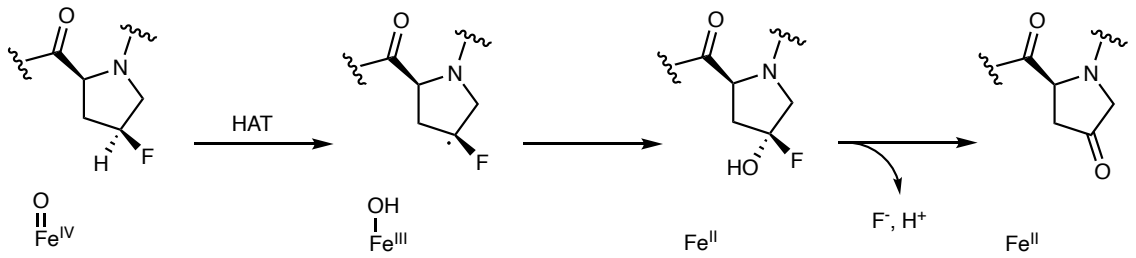

Figure 2-15. Hydroxylation-defluorination mechanism of nonheme iron 2-oxoglutarate dependent oxygenases. The oxoiron(IV) intermediate first activates a (sp^3)C-H bond in the substrate via HAT. Then, the substrate radical rebounds with the generated hydroxyl ligand and yields the aldehyde product via fluoride elimination.[34] Figure adapted from reference 34.

At this point, the source of the O atom in **3** needs to be identified first. Since the synthesis of **2** was carried out in drybox also, and in the trial where **3** was generated the solution-state work-up process took a long time, this may be an analogous case of the unexpected formation of $P(O)Ph_3$ from the PPh_4^+ in **1** as discussed above. Since now the protocol for preparing pure complex **2** has been developed, excess O_2 can be introduced into the acetonitrile or dichloromethane solution of **2**, and the reaction can be monitored using ^{19}F NMR. Usage of $^{18}O_2$ and tracking the product's isotopic incorporation with APCI mass spectrometry should also be considered.

Conclusion and Outlook

Novel tripodal-N_4 Cu complexes $(PPh_4)_2[Cu(N(o\text{-}PhNC(O)CF_3)_3)]$ (**1**) and $PPh_4[Cu(N(o\text{-}PhNC(O)CF_3)_3)]$ (**2**) were synthesized and characterized both in their solid-state and solution-state. Compared to previously reported tripodal-N_4 mononuclear Cu complexes supported by a neutral pyridine, amine, or imine ligand, the anionic amidate ligand $N(o\text{-}PhNHC(O)CF_3)_3$ ($\mathbf{H_3L^{CF3}}$) employed in this study results in unusual solid-state structural features of tripodal-N_4

Cu complexes: labiling effect that leads to a significantly long Cu-N_{ap} bond was observed in **1**, and an intramolecular fifth coordination of fluorine to the Cu center was seen in **2**.

Preliminary reactivity study of **1** with O_2 at room temperature indicates a pathway distinct from the Cu(I)→Cu(II)-superoxo transformation proposed in many Cu-centered oxygenases/oxidases and in precedent research on tripodal-N_4 Cu(I) complexes' reactivity toward O_2. Intriguingly, while simply exposing **1** to O_2 did not lead to an oxygenation of its countercation PPh_4^+, such a transformation was enabled with the addition of Et_4NCN. For complex **2**, although its oxidative reactivity has not been investigated, the isolation of its hydroxylation-defluorination product **3** suggests the potential of **2** to activate oxidants.

Clearly, the current study also raises many questions that prompt future work to be done:

- How exactly do **1** and **2** behave in solutions? What causes the difference in the electrochemical behavior of **1** in acetonitrile and dichloromethane, considering that it does not have the fifth solvent coordination? What are the species that disrupt the structure of **2** in acetonitrile and dichloromethane?
- What are the intermediates formed in the reaction between **1** and O_2? Do a Cu(II)-superoxo and/or Cu(II)-peroxo species form at a low temperature? Is there a Cu-O coordination? Is the ligand participating in the redox event(s) if there are any?
- What are the key intermediates that mediates the O-atom transfer from O_2 to PPh_4^+ in **1**? Why is Et_4NCN indispensable?
- What are the O-atom sources for the hydroxylation-defluorination product **3**? How does complex **2** activates these oxidants?

Viable approaches for tackling these problemes are proposed, and a pursuit of these questions would enable a thorough understanding of the oxidative reactivity of **1** and **2**, which will be the

knowledge foundation for developing them as effective oxidation catalysts. The discovery of the oxygenation of PPh_4^+ and the hydroxylation of a C-F bond, though fortuitous, does show promise in utilizing the two novel Cu complexes in mediating organic reactions of various types. Moreover, with the insights into the reactivity of **1** and **2**, further structure-function relationship studies can be conducted utilizing the variants of $\mathbf{H_3L^{CF3}}$. Previous studies have shown facile tuning of the acyl substituent on the family of amidate ligands with the successful incorporation of isopropyl, methyl, *tert*-butyl, and *tert*-butyl urea groups.[36] These can all effectively adjust the electronic and steric parameters of this series of amidate-based tripodal-N_4 ligands, allowing a comparison to be made with the previously discovered trends.

Experimental Section

General Considerations

All the manipulations that require an environment without O_2 and H_2O were conducted either using standard Schlenk techniques or conducted in an MBraun Labmaster 130 drybox under a nitrogen atmosphere. All reagents used were purchased from commercial vendors, and all anhydrous solvents were purchased from Sigma-Aldrich or were further purified by sparging with Ar gas followed by passage through activated alumina columns. X-ray diffraction studies were carried out in the X-ray Crystallography Laboratory at Emory University on a XtaLAB Synergy diffractometer. ^{1}H NMR spectra were recorded at room temperature on a INOVA 600 MHz and a Bruker 400 MHz spectrometer. Chemical shifts were referenced to residual solvents. ^{31}P NMR spectra were recorded at room temperature on a Bruker 600 MHz spectrometer with reverse gated decoupling. UV-vis absorption spectra were taken on a Shimadzu UV 3600 spectrophotometer using 1.0 cm quartz cuvettes. Mass spectra were recorded in the Mass Spectrometry Center at Emory University on a Thermo LTQ-FTMS mass spectrometer. Solid-state Infrared spectra were recorded as KBr pellets on a Varian Scimitar 800 Series FT-IR spectrophotometer. Cyclic voltammetry experiments were carried out using a CH Instruments (Austin, TX) Model 660C potentiostat. The three-component cell for carrying out the electrochemical experiments consisted of a glassy-carbon working electrode, a non-aqueous Ag/AgCl reference electrode, and a Pt wire counter electrode. All the reported electrochemical events are referenced versus the ferrocene/ferrocenium couple.

Synthesis of Ligand

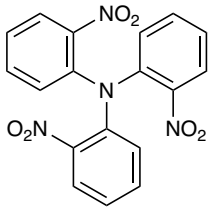

Tris(2-nitrophenyl)amine [N(*o*-PhNO$_2$)$_3$]. In a round bottom flask, 2-nitroaniline (5.0121 g, 0.0363 mol) and potassium carbonate (33.21 g, 0.24 mol) were dissolved in 30 mL dimethyl sulfoxide. After adding 1-fluoro-2-nitrobenzene (15.5 mL, 20.7 g, 0.147 mol), the reaction mixture was connected to N_2 and heated up to 150℃. Upon stirring for 91 h, the reaction was quenched by adding 500 mL DI water after cooling down to room temperature. The quenched reaction mixture was filtered through a medium-porosity glass frit, and brown solid was isolated. The crude product was then added to 500mL of boiling methanol and stirred for 20 min. Filtering the methanol suspension hot via a medium-porosity glass frit yielded yellow solid as the product, which was further purified through recrystallization via slow evaporation of its concentrated dichloromethane solution (6.012 g, 44%). The crystalline product was dried under vacuum for 5 h. ^{1}H NMR (400 MHz, $CDCl_3$): δ 7.83 (3H, d), 7.53 (3H, t), 7.30 (3H, t), 7.21 (3H, d).

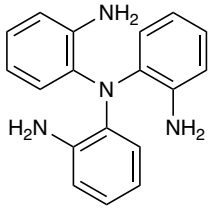

Tris(2-aminophenyl)amine [N(*o*-PhNH$_2$)$_3$]. In a pressure safe reaction bottle N(*o*-PhNO$_2$)$_3$ (2.9995 g, 0.0079 mol) was suspended in 15 mL tetrahydrofuran. After adding 5% Pd/C (1.6817 g, 10 mol%), the reaction mixture was connected to a hydrogenator immediately and shaken under an H_2 atmosphere (50 psi) for 2 h. The reaction mixture was then quickly filtered through a pad of celite on a medium-porosity glass frit. The filtrate was concentrated in vacuo to yield a

pale pink solid. The solid was washed with 30 mL of diethyl ether three times to isolate an off-white solid. The diethyl ether filtrate was then evaporated and re-filtered three times to isolate more solids. All the solids were combined, transferred into the drybox, and re-dissolved in a minimum amount of tetrahydrofuran. The product was isolated as colorless crystals (0.82 g, 36%) upon layer diffusion of hexane into the concentrated tetrahydrofuran solution and dried under vacuum for 6 h. ^{1}H NMR (400 MHz, $CDCl_3$): δ 6.99 (3H, t), 6.91 (3H, d), 6.73 (3H, d), 6.70 (3H, t), 2.78 (6H, bs).

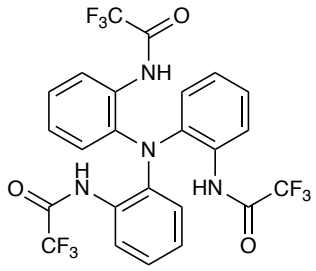

2, 2‘, 2‘‘-Tris(trifluoroamido)triphenylamine [N(*o*-PhNHC(O)CF_3)$_3$]. In a round bottom flask, N(*o*-$PhNH_2$)$_3$ (0.78 g, 0.003 mol) was suspended in 12.5 mL dichloromethane. After the reaction mixture was connected to N_2 and cooled to 0℃, triethylamine (1.38 mL, 1.00 g, 0.01 mol) was added. Trifluoroacetic anhydride (1.25 mL, 1.89 g, 0.01 mol) was then added dropwise to the mixture. After stirring for 15 min at 0℃, the reaction mixture was warmed to room temperature and stirred for another 1.5 h. The reaction was washed three times with saturated sodium bicarbonate solution (15 mL) and three times with DI water (15 mL). The pale brown organic layer was dried over magnesium sulfate and concentrated in vacuo to yield a tan oil. The oil was then triturated with 50 mL boiling hexane to yield the off-white product (1.2018 g, 75%). The product was dried under vacuum for 22 h. ^{1}H NMR (400 MHz, $CDCl_3$): δ 8.51 (3H, bs), 7.68 (3H, d), 7.23 (6H, m), 6.88 (3H, d).

Synthesis of Copper Complexes

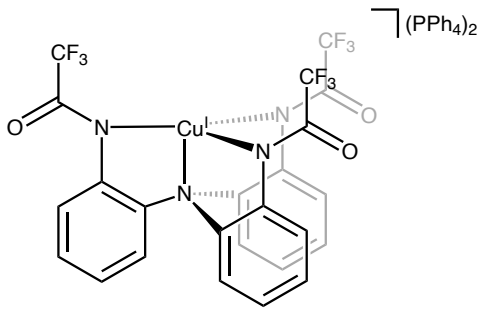

$(PPh_4)_2$[Cu(N(*o*-PhNC(O)CF_3)$_3$)] (1). In the drybox, N(*o*-PhNHC(O)CF_3)$_3$ (302 mg, 0.522 mmol) was dissolved in 10 mL dimethylformamide in a 20 mL disposable vial. Then potassium hydride (67.4 mg, 1.68 mmol) was added. After stirring the reaction mixture for 30 min, copper(I) bromide (74.9 mg, 0.522 mmol) and tetraphenylphosphonium bromide (435.8 mg, 1.039 mmol) were added to the reaction mixture in sequence. Upon stirring for another 24 h, the reaction mixture was concentrated in vacuo. Acetonitrile (5 mL) was then added to the reaction mixture. After filtration over a medium-porosity glass frit, an off-white solid and a golden yellow filtrate were obtained. The filtrate was concentrated in vacuo and re-dissolved in a minimum amount of acetonitrile. Diethyl ether was layered on top of the concentrated acetonitrile solution, and the product was isolated in a crystalline form after 12 h (477.9 mg, 70% yield). X-ray diffraction quality crystals were obtained by vapor evaporation of diethyl ether into a concentrated solution of **1** in acetonitrile. **^{1}H NMR** (CD_3CN, 600 MHz): δ 7.91 (td, *J* = 7.3, 1.8 Hz, 8H), 7.78 – 7.64 (m, 35H), 6.95 (dd, *J* = 7.8, 1.8 Hz, 3H), 6.90 – 6.85 (m, 3H), 6.71 (td, *J* = 7.6, 1.8 Hz, 3H). **^{1}H NMR** (CD_2Cl_2, 400 MHz): δ 7.94 – 7.83 (m, 8H), 7.75 – 7.64 (m, 19H), 7.67 – 7.52 (m, 19H), 6.89 (dd, *J* = 7.8, 1.6 Hz, 3H), 6.82 – 6.73 (m, 3H), 6.61 (td, *J* = 7.4, 1.6 Hz, 3H). **^{13}C NMR** (CD_3CN, 600 MHz): 159.23, 159.03, 158.83, 148.23, 144.09, 136.36, 136.34, 135.70, 135.63, 135.43, 131.33, 131.25, 128.23, 125.74, 124.23, 122.96, 121.10, 120.94, 119.20, 119.03, 118.60, 118.26, 66.23, 15.58, 1.72, 1.69, 1.55, 1.41, 1.27, 1.14, 1.00, 0.86.

IR (KBr, cm^{-1}): υ(CO) = 1619; **HRMS** (-ESI): calculated for $C_{24}H_{12}CuF_9N_4O_3$ 638.01, found 639.02.

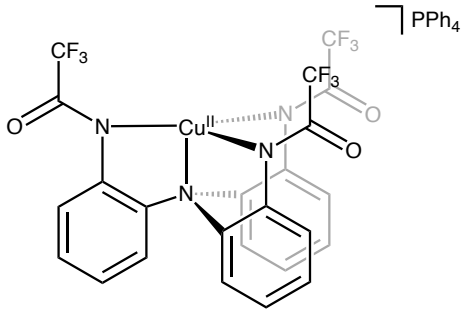

PPh_4[Cu(N(*o*-PhNC(O)CF_3)$_3$)] (2). In the drybox, N(*o*-PhNHC(O)CF_3)$_3$ (300mg, 0.519 mmol) was dissolved in 10 mL dimethylformamide in a 20 mL disposable vial. Then potassium hydride (65.8 mg, 1.64 mmol) was added. After stirring the reaction mixture for 30 min, copper(II) bromide (115.9 mg, 0.519 mmol) and tetraphenylphosphonium bromide (216.8 mg, 0.517 mmol) were added to the reaction mixture in sequence. Upon stirring for another 24 h, the reaction mixture was concentrated in vacuo. Acetonitrile (4 mL) was then added to the reaction mixture. After filtration over a medium-porosity frit, an off-white solid and a golden yellow filtrate were obtained. The filtrate was concentrated in vacuo and re-dissolved in a minimum amount of dichloromethane. Hexane was layered on top of the concentrated dichloromethane solution, and the product (X-ray diffraction quality crystals) was isolated after 12 h (413.1 mg, 82% yield). **IR** (KBr, cm^{-1}): υ(CO) = 1644; **HRMS** (-ESI): calculated for $C_{24}H_{12}CuF_9N_4O_3$ 638.01, found 639.01.

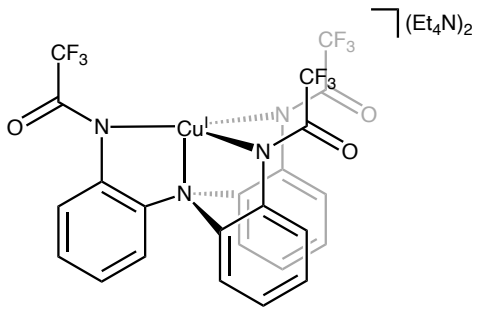

$(Et_4N)_2$[Cu(N(*o*-PhNC(O)CF_3)$_3$)] (1'). Same procedure was followed as the synthesis of **1** except for adding tetraethylammonium bromide instead of tetraphenylphosphonium bromide. In the work-up, after the reaction mixture was concentrated in vacuo, it was fully dissolved in acetonitrile, stirred for 12 h, and then filtered. X-ray diffraction quality crystals were obtained by vapor evaporation of diethyl ether into a concentrated solution of **1'** in acetonitrile. Since only tiny amounts of product were isolated, its yield was not calculated.

*Reaction of **1** with Tetraethylammonium Cyanide in Drybox (Initial Trial)*

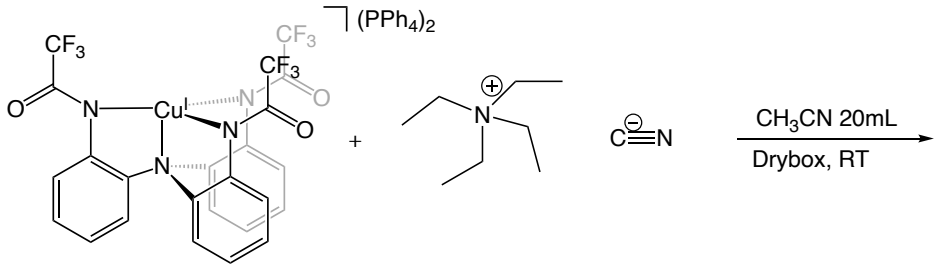

Complex **1** (88.5 mg, 0.067 mmol) was dissolved in 20 mL acetonitrile in a 20 mL disposable vial. Upon the addition of tetraethylammonium cyanide (10.2 mg, 0.065 mmol), the color of the reaction mixture immediately darkened. After stirring for three days, white precipitate was observed. After filtering the reaction mixture through a medium porosity glass frit, the filtrate was washed with toluene and filtered again. The filtrate was dried in vacuo and washed with pentane, generating a pentane solution and trace amounts of red oil drops. X-ray diffraction quality crystals of $P(O)Ph_3$ were obtained through slow evaporation of pentane.

*Reaction of **1** with Tetraethylammonium Cyanide in Drybox (^{31}P NMR Measurement)*

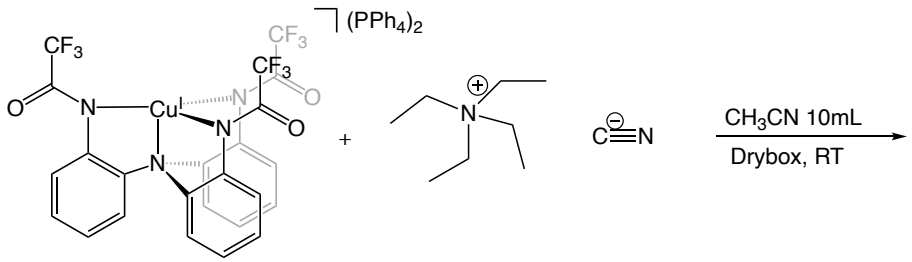

Complex **1** (45.1 mg, 0.034 mmol) was dissolved in 10 mL acetonitrile in a 20 mL disposable vial and then tetraethylammonium cyanide (5.7 mg, 0.036 mmol) was added. An aliquot (0.6 mL) of the reaction mixture was transferred into an NMR tube, mixed with deuterated acetonitrile (0.06 mL), sealed, and taken out of the drybox for ^{31}P NMR measurement. Measurements were made 37 min, 87 min, and 242 min after the reaction started.

*Reaction of **1** with Tetraethylammonium Cyanide Under Excess O_2 (^{31}P NMR Measurement)*

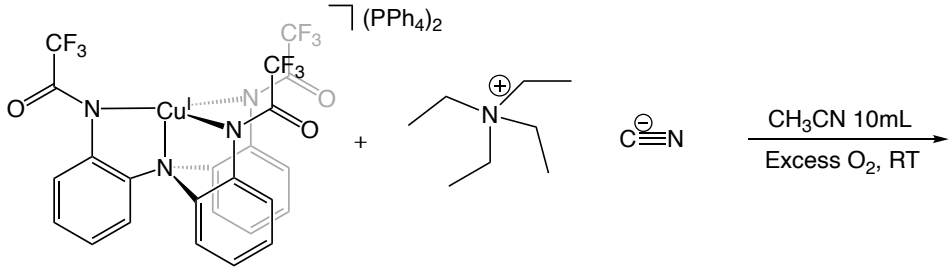

Complex **1** (46.0 mg, 0.035 mmol) was dissolved in 10 mL acetonitrile in a 25 mL round bottom flask and then tetraethylammonium cyanide (5.6 mg, 0.036 mmol) was added. The reaction vessel was quickly sealed and taken out of the drybox. The reaction was connected to the O_2 tube 12 min after the mixing of **1** and tetraethylammonium cyanide (when reaction started). An aliquot (0.6 mL) of the reaction mixture was transferred into an NMR tube, mixed with deuterated acetonitrile (0.06 mL), and taken for ^{31}P NMR measurement. Measurements were made 32 min, 95 min, and 263 min after the reaction started.

*Reaction of **1** Under Excess O_2 without Tetraethylammonium Cyanide (^{31}P NMR Measurement)*

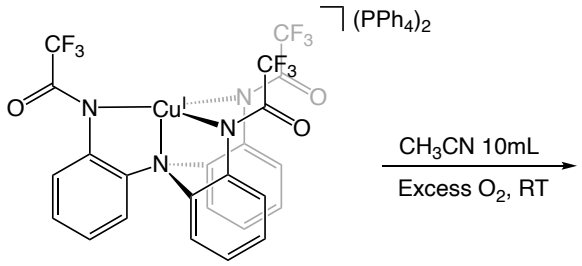

Complex **1** (46.9 mg, 0.036 mmol) was dissolved in 10 mL acetonitrile in a 25 mL round bottom flask. The reaction vessel was quickly sealed and taken out of the drybox. The reaction was connected to the O_2 tube 13 min after the dissolving **1** in acetonitrile (when reaction started). An aliquot (0.6 mL) of the reaction mixture was transferred into an NMR tube, mixed with deuterated acetonitrile (0.06 mL), and taken for ^{31}P NMR measurement. Measurements were made 30 min, 108 min, and 286 min after the reaction started.

Reference

1. Jones, M. B.; MacBeth, C. E., Tripodal Phenylamine-Based Ligands and Their CoII Complexes. *Inorganic Chemistry* **2007,** *46* (20), 8117-8119.

2. Paraskevopoulou, P.; Ai, L.; Wang, Q.; Pinnapareddy, D.; Acharyya, R.; Dinda, R.; Das, P.; Çelenligil-Çetin, R.; Floros, G.; Sanakis, Y.; Choudhury, A.; Rath, N. P.; Stavropoulos, P., Synthesis and Characterization of a Series of Structurally and Electronically Diverse Fe(II) Complexes Featuring a Family of Triphenylamido-Amine Ligands. *Inorganic Chemistry* **2010,** *49* (1), 108-122.

3. Eckenhoff, W. T.; Pintauer, T., Structural Comparison of Copper(I) and Copper(II) Complexes with Tris(2-pyridylmethyl)amine Ligand. *Inorganic Chemistry* **2010,** *49* (22), 10617-10626.

4. Raab, V.; Kipke, J.; Burghaus, O.; Sundermeyer, J., Copper Complexes of Novel Superbasic Peralkylguanidine Derivatives of Tris(2-aminoethyl)amine as Constraint Geometry Ligands. *Inorganic Chemistry* **2001,** *40* (27), 6964-6971.

5. Becker, M.; Heinemann, F. W.; Schindler, S., Reversible Binding of Dioxygen by a Copper (I) Complex with Tris (2-dimethylaminoethyl) amine (Me6tren) as a Ligand. *Chemistry–A European Journal* **1999,** *5* (11), 3124-3129.

6. Schatz, M.; Becker, M.; Thaler, F.; Hampel, F.; Schindler, S.; Jacobson, R. R.; Tyeklár, Z.; Murthy, N. N.; Ghosh, P.; Chen, Q.; Zubieta, J.; Karlin, K. D., Copper(I) Complexes, Copper(I)/O2 Reactivity, and Copper(II) Complex Adducts, with a Series of Tetradentate Tripyridylalkylamine Tripodal Ligands. *Inorganic Chemistry* **2001,** *40* (10), 2312-2322.

7. Wei, N.; Murthy, N. N.; Chen, Q.; Zubieta, J.; Karlin, K. D., Copper(I)/Dioxygen Reactivity of Mononuclear Complexes with Pyridyl and Quinolyl Tripodal Tetradentate Ligands: Reversible Formation of Cu:O2 = 1:1 and 2:1 Adducts. *Inorganic Chemistry* **1994,** *33* (9), 1953-1965.

8. Brückmann, T.; Becker, J.; Turke, K.; Smarsly, B.; Weiß, M.; Marschall, R.; Schindler, S., Immobilization of a copper complex based on the tripodal ligand (2-aminoethyl)bis(2-pyridylmethyl)amine (uns-penp). *Zeitschrift für anorganische und allgemeine Chemie* **2021,** *647* (5), 560-571.

9. Patra, Goutam K.; Goldberg, I., Syntheses and Crystal Structures of Copper and Silver Complexes with New Imine Ligands − Air-Stable, Photoluminescent CuIN4 Chromophores. *European Journal of Inorganic Chemistry* **2003,** *2003* (5), 969-977.

10. Shi, Q.; Thatcher, R. J.; Slattery, J.; Sauari, P. S.; Whitwood, A. C.; McGowan, P. C.; Douthwaite, R. E., Synthesis, Coordination Chemistry and Bonding of Strong N-Donor Ligands Incorporating the 1H-Pyridin-(2E)-Ylidene (PYE) Motif. *Chemistry – A European Journal* **2009,** *15* (42), 11346-11360.

11. Will, J.; Würtele, C.; Becker, J.; Walter, O.; Schindler, S., Synthesis, crystal structures and reactivity towards dioxygen of copper(I) complexes with tripodal aliphatic amine ligands. *Polyhedron* **2019,** *171*, 448-454.

12. Muthuramalingam, S.; Anandababu, K.; Velusamy, M.; Mayilmurugan, R., Benzene Hydroxylation by Bioinspired Copper(II) Complexes: Coordination Geometry versus Reactivity. *Inorganic Chemistry* **2020,** *59* (9), 5918-5928.

13. Masahiro, M.; Sigeo, K.; Ichiro, M., Crystal and Molecular Structures of [Cu2(taec)X](ClO4)3·nH2O (taec=N,N′,N″,N‴-Tetrakis(2-aminoethyl)-1,4,8,11-

tetraazacyclotetradecane; X=I, F, NO2, and CH3COO; n=0, 1, or 2). Effect of Incorporation of an Anion X on the Structure of the Complex Cation. *Bulletin of the Chemical Society of Japan* **1987,** *60* (5), 1681-1689.

14. Reger, D. L.; Foley, E. A.; Watson, R. P.; Pellechia, P. J.; Smith, M. D.; Grandjean, F.; Long, G. J., Monofluoride Bridged, Binuclear Metallacycles of First Row Transition Metals Supported by Third Generation Bis(1-pyrazolyl)methane Ligands: Unusual Magnetic Properties. *Inorganic Chemistry* **2009,** *48* (22), 10658-10669.

15. Reger, D. L.; Pascui, A. E.; Smith, M. D.; Jezierska, J.; Ozarowski, A., Dinuclear Complexes Containing Linear M–F–M [M = Mn(II), Fe(II), Co(II), Ni(II), Cu(II), Zn(II), Cd(II)] Bridges: Trends in Structures, Antiferromagnetic Superexchange Interactions, and Spectroscopic Properties. *Inorganic Chemistry* **2012,** *51* (21), 11820-11836.

16. Royzen, M.; Wilson, J. J.; Lippard, S. J., Physical and structural properties of [Cu(BOT1)Cl]Cl, a fluorescent imaging probe for HNO. *Journal of Inorganic Biochemistry* **2013,** *118*, 162-170.

17. Elgrishi, N.; Rountree, K. J.; McCarthy, B. D.; Rountree, E. S.; Eisenhart, T. T.; Dempsey, J. L., A Practical Beginner's Guide to Cyclic Voltammetry. *Journal of Chemical Education* **2018,** *95* (2), 197-206.

18. Jacobson, R. R.; Tyeklar, Z.; Farooq, A.; Karlin, K. D.; Liu, S.; Zubieta, J., A copper-oxygen (Cu2-O2) complex. Crystal structure and characterization of a reversible dioxygen binding system. *Journal of the American Chemical Society* **1988,** *110* (11), 3690-3692.

19. Kwon, H.; Lee, E., Static and dynamic coordination behaviours of copper(i) ions in hexa(2-pyridyl)benzene ligand systems. *Dalton Transactions* **2018,** *47* (25), 8448-8455.

20. Mehlich, F.; Roberts, A. E.; Kerscher, M.; Comba, P.; Lawrance, G. A.; Würtele, C.; Becker, J.; Schindler, S., Synthesis and characterization of copper complexes with a series of tripodal amine ligands. *Inorganica Chimica Acta* **2019,** *486*, 742-749.

21. Broge, L.; Pretzmann, U.; Jensen, N.; Søtofte, I.; Olsen, C. E.; Springborg, J., Cobalt(II), Nickel(II), Copper(II), and Zinc(II) Complexes with [35]Adamanzane, 1,5,9,13-Tetraazabicyclo[7.7.3]nonadecane, and [(2.3)2.21]Adamanzane, 1,5,9,12-Tetraazabicyclo[7.5.2]hexadecane. *Inorganic Chemistry* **2001,** *40* (10), 2323-2334.

22. Karlin, K. D.; Wei, N.; Jung, B.; Kaderli, S.; Zuberbuehler, A. D., Kinetic, thermodynamic, and spectral characterization of the primary copper-oxygen (Cu-O2) adduct in a reversibly formed and structurally characterized peroxo-dicopper(II) complex. *Journal of the American Chemical Society* **1991,** *113* (15), 5868-5870.

23. Weitzer, M.; Schindler, S.; Brehm, G.; Schneider, S.; Hörmann, E.; Jung, B.; Kaderli, S.; Zuberbühler, A. D., Reversible Binding of Dioxygen by the Copper(I) Complex with Tris(2-dimethylaminoethyl)amine (Me6tren) Ligand. *Inorganic Chemistry* **2003,** *42* (6), 1800-1806.

24. Schatz, M.; Raab, V.; Foxon, S. P.; Brehm, G.; Schneider, S.; Reiher, M.; Holthausen, M. C.; Sundermeyer, J.; Schindler, S., Combined Spectroscopic and Theoretical Evidence for a Persistent End-On Copper Superoxo Complex. *Angewandte Chemie International Edition* **2004,** *43* (33), 4360-4363.

25. Kobayashi, Y.; Ohkubo, K.; Nomura, T.; Kubo, M.; Fujieda, N.; Sugimoto, H.; Fukuzumi, S.; Goto, K.; Ogura, T.; Itoh, S., Copper(I)-Dioxygen Reactivity in a Sterically Demanding Tripodal Tetradentate tren Ligand: Formation and Reactivity of a Mononuclear Copper(II) End-On Superoxo Complex. *European Journal of Inorganic Chemistry* **2012,** *2012* (29), 4574-4578.

26. Paria, S.; Morimoto, Y.; Ohta, T.; Okabe, S.; Sugimoto, H.; Ogura, T.; Itoh, S., Copper(I)–Dioxygen Reactivity in the Isolated Cavity of a Nanoscale Molecular Architecture. *European Journal of Inorganic Chemistry* **2018,** *2018* (19), 1976-1983.

27. Schatz, M.; Becker, M.; Walter, O.; Liehr, G.; Schindler, S., Reactivity towards dioxygen of a copper(I) complex of tris(2-benzylaminoethyl)amine. *Inorganica Chimica Acta* **2001,** *324* (1), 173-179.

28. Schneider, L.; Becker, J.; Schindler, S., Investigations of metal complexes with the tripodal tetradentate ligand tris(2-(propan-2-ylideneamino)ethyl)amine (imine3tren). *Zeitschrift für anorganische und allgemeine Chemie* **2021,** *647* (11), 1139-1144.

29. Deng, Z.; Lin, J.-H.; Xiao, J.-C., Nucleophilic arylation with tetraarylphosphonium salts. *Nature Communications* **2016,** *7* (1), 10337.

30. Lim, B. S.; Holm, R. H., Molecular Heme−Cyanide−Copper Bridged Assemblies: Linkage Isomerism, Trends in νCN Values, and Relation to the Heme-a3/CuB Site in Cyanide-Inhibited Heme−Copper Oxidases. *Inorganic Chemistry* **1998,** *37* (19), 4898-4908.

31. Kang, S.-G.; Song, J.; Jeong, J. H., Syntheses and characterization of mono- and di-N-hydroxyethylated tetraaza macrocycles containing eight C-methyl groups and their nickel(II) and copper(II) complexes. *Inorganica Chimica Acta* **2000,** *310* (2), 196-202.

32. Horn, A.; Fernandes, C.; Bortoluzzi, A. J.; Vugman, N. V.; Herbst, M. H., Coordination chemistry of the new ligand 1-(bis-pyridin-2-ylmethyl-amino)-3-chloropropan-2-ol (HPClNOL) with copper(II). X-ray crystal structure, spectroscopic and electrochemical properties of the complex [Cu(HPClNOL)(CH3CN)](ClO4)2. *Journal of Molecular Structure* **2005,** *749* (1), 96-102.

33. Sivanesan, D.; Seo, B.; Lim, C.-S.; Kim, H.-G., Facile hydrogenation of bicarbonate to formate in aqueous medium by highly stable nickel-azatrane complex. *Journal of Catalysis* **2020,** *382*, 121-128.

34. Costas, M.; Company, A., Oxidative C−F Cleavage in Metalloenzymes and Model Compounds. *European Journal of Inorganic Chemistry* **2022,** *2022* (1), e202100754.

35. Besalú-Sala, P.; Magallón, C.; Costas, M.; Company, A.; Luis, J. M., Mechanistic Insights into the ortho-Defluorination-Hydroxylation of 2-Halophenolates Promoted by a Bis(μ-oxo)dicopper(III) Complex. *Inorganic Chemistry* **2020,** *59* (23), 17018-17027.

36. Liu, D. Development of Bis(amidophenyl)amine Redox-active Ligands for Multi-electron Catalysis by Transition Metals Emory University, 2020.